Journal of Statistical Physics, Vol. 91, Nos. 1/2, 1998

Predictive Turbulence Modeling by Variational Closure

Gregory L. Eyink[1] and Francis J. Alexander[2]

Received July 8, 1997; final January 28, 1998

We show that a variational implementation of probability density function (PDF) closures has the potential to make predictions of general turbulence mean statistics for which *a priori* knowledge of the incorrectness is possible. This possibility exists because of realizability conditions on "effective potential" functions for general turbulence statistics. These potentials measure the cost for fluctuations to occur away from the ensemble-mean value in empirical time-averages of the given variable, and their existence is a consequence of a refined ergodic hypothesis for the governing dynamical system (Navier–Stokes dynamics). Approximations of the effective potentials can be calculated within PDF closures by an efficient Rayleigh–Ritz algorithm. The failure of realizability within a closure for the approximate potential of any chosen statistic implies *a priori* that the closure prediction for that statistic is not converged. The systematic use of these novel realizability conditions within PDF closures is shown in a simple 3-mode system of Lorenz to result in a statistically improved predictive ability. In certain cases the variational method allows an *a priori* optimum choice of free parameters in the closure to be made.

KEY WORDS: Nonequilibrium dynamics; turbulence; variational principle; statistical closure; modeling.

1. INTRODUCTION

Despite a century or more of effort in the modeling of turbulent flows since the pioneering works of Boussinesq[1] and Reynolds,[2] it seems fair to say that predictive methods are still not available. An excellent review of the modeling research up to modern times is given by Speziale.[3] The main

[1] Department of Mathematics, University of Arizona, Tucson, Arizona 85721; e-mail: eyink@math.arizona.edu.

[2] Center for Computational Science, Boston University, Boston, Massachusetts 02215; e-mail: fja@buphyk.bu.edu.

0022-4715/98/0400-0221$15.00/0

conclusion may be stated as follows: Because there is no clear-cut separation of time- or length-scales in turbulent flows and no small parameter for expansion in nonlinearity, it is impossible to derive systematically equations of motions for averages by statistical methods, unlike some other areas, such as kinetic theory of gases. While models adequate to reproduce experimental data for many given flow conditions have been devised, the resulting closures are notoriously unreliable when applied to new situations. In other words, the models are really only *postdictive*. By this we mean that the models can, with appropriate adjustment of parameters, be made to yield reasonable fits to *existing* data from experiment or simulation. However, this is of very limited use from a practical point of view, because in actual engineering problems one is interested to employ the theory precisely to predict new regimes. If experimental or simulation data were readily available, then there would be little need for the theory! For example, in aeronautical engineering the closure models may be used at most as a crude guide for actual design, which must then be refined in subsequent expensive testing, either by putting scale models in wind tunnels or by test piloting. An optimistic appraisal of the current approach to turbulence modeling—which we believe warranted—is that it does yield some insight into the basic physics of the turbulent flows. However, a more pessimistic point of view having also some justification is that the existing turbulence models are little more than sophisticated summaries of the databases from which their parameters are determined. It is not possible to make truly reliable predictions from such models. In general, it is impossible to say *a priori* whether the deductions from such models are in close agreement to reality or very far from the truth.

One exception to this general rule is for turbulence statistics which satisfy a *realizability* condition arising from the positivity of the statistical distributions over turbulent flow realizations. Examples are second-order statistics such as energy spectra and Reynolds stresses, which inherit positivity properties from the underlying distributions. To our knowledge, the recognition of the importance of such realizability conditions and their systematic exploitation in turbulence modeling is due to Kraichnan[4, 5] (see also ref. 6). Realizability has also been introduced as a fundamental constraint in Reynolds-stress closures by Schumann[7] and Lumley.[8] A turbulence model prediction which violates such a realizability condition is necessarily badly in error for that statistic. Unfortunately, this tool is only of limited usefulness since the first-order turbulence statistics of greatest engineering interest—such as mean velocity or pressure profiles—do not possess obvious realizability constraints. Furthermore, relatively crude models of the second-order statistics (which *are* limited by realizability conditions) may suffice to give adequate predictions of the first-order

statistics. Thus, a failure of realizability for the second-order statistics, especially if it occurred in a remote wavenumber range or for peculiar flow situations, need not imply that the model predictions for first-order statistics are badly in error.

Our purpose in this paper is threefold:

First, we shall explain that *there are realizability conditions associated to all turbulence statistics, including first-order quantities such as mean velocity profiles.* These realizability conditions result from a refinement of the standard ergodic hypothesis. According to this refinement, empirical averages over a finite time-series of the given variable will have fluctuations away from the ensemble-mean value whose probability decays exponentially in the duration (or length) of the series. The rate of decay in the statistical steady-state is governed by a so-called *effective potential*, which is a function of the possible values of the considered variable. Realizability requires that this potential function be nonnegative, convex and vanish only at the ensemble-average value. These effective potential functions are also closely connected with ideas of Onsager[9] on action principles for nonequilibrium fluctuations. This theory has been discussed earlier in refs. 10 and 11.

The second goal of this paper is to show that *there is a practical, efficient method to calculate approximations to the effective potential within PDF-based moment closures, via a Rayleigh–Ritz variational scheme.* PDF-based closures, such as the mapping closures,[12, 13] the generalized Langevin models,[14, 15] Fokker–Planck closures,[16] etc. have been developed particularly in the last decade as more complete models of turbulent flow than traditional moment-closures. They contain much more statistical information about the random fields and, in particular, suffice to recover the effective potential function. The Rayleigh–Ritz method for that purpose has been discussed previously.[10, 11] It has also been shown in a simple Langevin model to yield a computationally convergent scheme for the exact effective potential.[17] As we shall show here, the variational scheme can also, in favorable cases, determine *a priori* an optimum value of free parameters within the closure, i.e. independent of fitting to empirical data.

Our final, and main, purpose in this work will be to show that *the satisfaction or failure of the realizability conditions on the approximate effective potential is a sensitive diagnostic of the reliability of the closure prediction for the average of the particular variable considered.* To be precise, nothing can be inferred if the effective potential realizability conditions are satisfied within the closure: the predictions may then be either good or bad (just as with traditional realizability conditions). However, failure of realizability of the approximate potential will be seen to imply that the closure prediction is poor for the considered variable. This will be argued

from the relation of the effective potential to the fluctuations of the given random variable. It will also be demonstrated by concrete computations in a simple 3-mode caricature of the Navier–Stokes dynamics, first considered by Lorenz. Some of these results have been briefly reported elsewhere.[18]

To keep things simple and concrete, all of the closures considered in this work will be for this same system of Lorenz.[19] The dynamics is defined for three real variables x_i, $i=1, 2, 3$ via the stochastic differential equations

$$\dot{x}_i = A_i x_j x_k - \nu_i x_i + f_i \tag{1}$$

with i, j, k a cyclic permutation of 1, 2, 3, with interaction coefficients A_i, $i=1, 2, 3$ subject to the constraint

$$A_1 + A_2 + A_3 = 0 \tag{2}$$

guaranteeing conservation of energy $E = \frac{1}{2}\sum_i x_i^2$ by the nonlinear terms, with positive damping coefficients $\nu_i > 0$, $i=1, 2, 3$ and with f_i, $i=1, 2, 3$ random Gaussian forces of zero means and covariance

$$\langle f_i(t)\, f_j(t')\rangle = 2\kappa_i \delta_{ij}\, \delta(t-t') \tag{3}$$

for $\kappa_i > 0$, $i=1, 2, 3$, i.e. white-noise in time. This model has been often used before as a simple first test of turbulence closure ideas: DIA,[20] resummed perturbation theory schemes,[21] and Wiener–Hermite expansion methods.[22] The advantage is that the ideas may be cleanly tested in a situation where direct numerical simulation (DNS) of the dynamics is trivial. As we shall see in the main body of this paper, the new realizability conditions perform very well as closure diagnostics in this simple model. This motivates the exploration of their effectiveness in PDF closures for Navier–Stokes turbulence, which we have now underway.

Assuming that similar results hold for Navier–Stokes dynamics, we believe that this points toward significant new directions in turbulence modeling. In the first place, there is a now a practical impetus to pursue PDF-based closures, both to develop further the existing PDF methods[12, 13, 14, 15] and to explore new ones. For example, the "synthetic turbulence" models of ref. 23 may be a promising avenue to explore. In fact, these methods seem to be the only ones with a potential to have real predictive power. Note that the new realizability conditions on effective potentials used in conjunction with PDF closures cannot eliminate the need for *a posteriori* testing of the closure predictions. Since even poor predictions might be consistent with realizability, it would be most unwise to use any kind of realizability condition as a sole check of the closure.

However, applied as an *a priori* "screening" of closures, the realizability check on effective potentials might detect a sizable fraction of poor predictions in advance and thus reduce the need for subsequent expensive testing, design refinement, etc. In this way, the effective potential realizability check could have great economizing capability, particularly if the check is easy and cheap itself to perform. The method proposed should, in short, result in a *statistically-improved predictive ability*, i.e. a greater fraction of turbulence closure predictions which pass the "screening" should be accurate. The challenge is then to develop PDF-based closure methods which incorporate such checks and which, at the same time, are adequate to describe the desired range of phenomena.

The precise contents of this work are as follows: In the following Section 2 we briefly review the theory of the refined ergodic hypothesis and the properties of the associated effective potential function. We also review there the Rayleigh–Ritz method of computation and its relation to PDF-based moment closures. With this as background, we consider in Sections 3–5 three distinct PDF closures for the previous 3-mode model, namely, truncated Hermite-polynomial expansions, a "chi-square" *Ansatz*, and a "twisted-Gaussian" *Ansatz*. In particular, closure predictions for various statistics shall be computed and compared with DNS of the models, and as well the Rayleigh–Ritz effective potentials for those statistics shall be computed. In the conclusion, Section 6, the results will be reviewed and some general directions for future work discussed. There are finally a series of Appendices that contain some information auxiliary to the main text. The Appendix I discusses some of the properties of the 3-mode dynamics, Eq. (1), and its statistical solutions. In Appendix II some technical results are given on optimization over parameters. Finally, in Appendix III there are listed various quantities in the PDF closures considered, which are used in the numerical calculation of the effective potentials.

2. THE EFFECTIVE POTENTIAL AND THE RAYLEIGH–RITZ METHOD

2.1. The Refined Ergodic Hypothesis and Effective Potential

We shall now briefly discuss the refined ergodic hypothesis and the role of the effective potential in that theory. A more detailed account has already been given in refs. 10 and 11, so that we can be rather brief here. Consider any chosen set of random variables $\mathbf{W} = (W_1, W_2, \ldots, W_N)$. These could be x-components of velocity $W_i = u(\mathbf{r}_i)$ at some selected set of

points $\mathbf{r}_i$, $i=1,...,N$ in a turbulent flow, or they could be instead the square velocity fluctuations $W_i=(\mathbf{v}'(\mathbf{r}_i))^2$, with $\mathbf{v}'(\mathbf{r}_i)\equiv\mathbf{v}(\mathbf{r}_i)-\bar{\mathbf{v}}(\mathbf{r}_i)$, in the same flow, etc. *Any* random variable of interest may be considered and the remarks we make here are completely general. Let us introduce the empirical *time-average*

$$\bar{\mathbf{W}}_T\equiv\frac{1}{T}\int_0^T dt\,\mathbf{W}(t) \tag{4}$$

over the time-series $\mathbf{W}(t)$ of duration T. Of course, the standard ergodic hypothesis states that, with probability $=1$ in each realization of the system,

$$\lim_{T\to\infty}\bar{\mathbf{W}}_T=\bar{\mathbf{w}} \tag{5}$$

where $\bar{\mathbf{w}}=\langle\mathbf{W}\rangle$ is the *ensemble-average* value of the set of random variables. This hypothesis has never been proved for Navier–Stokes turbulence, but it is quite generally accepted as valid (e.g. see Sections 3.3 and 4.7 of ref. 24, or Section 4.4 of ref. 25). We now propose the following *refined ergodic hypothesis* that

$$\mathrm{Prob}\{\bar{\mathbf{W}}_T\approx\mathbf{w}\}\sim\exp(-T\cdot V[\mathbf{w}]), \tag{6}$$

where $\mathrm{Prob}\{\bar{\mathbf{W}}_T\approx\mathbf{w}\}$ is the probability that the empirical average $\bar{\mathbf{W}}_T$ over time-interval $[0, T]$ takes on the value $=\mathbf{w}$ and $V[\mathbf{w}]$ is a certain non-negative function of the possible values. It is assumed that $V[\bar{\mathbf{w}}]=0$ but that $V[\mathbf{w}]>0$ for $\mathbf{w}\neq\bar{\mathbf{w}}$. This refined hypothesis states that for large T there will be an exponentially small probability to observe any value $\mathbf{w}$ of the time-average distinct from the ensemble-mean value $\bar{\mathbf{w}}$. In other words, it states not only that the time-average will be equal to the ensemble-average with high probability for large T, but it also gives a quantitative estimate on the (very small) probability of deviations. The above statement of the hypothesis is somewhat heuristic. A more precise formulation is that the following limits should exist

$$\lim_{\delta\to 0}\lim_{T\to\infty}\frac{1}{T}\log\mathrm{Prob}\{|\mathbf{W}_T-\mathbf{w}|\leqslant\delta\}=-V[\mathbf{w}], \tag{7}$$

for every $\mathbf{w}$, with some function V having the properties stated above.

There are several considerations that motivate the above hypothesis for Navier–Stokes turbulence. First, for a wide class of ergodic Markov

processes the above hypothesis has been proved as a rigorous theorem in the so-called *large-deviations theory* of Donsker and Varadhan (e.g., see ref. 26). The class of systems covered by this theory are random processes or stochastic dynamics, governed for example by stochastic differential equations (such as our Eq. (1)). On the other hand, the hypothesis has also been proved to be valid in deterministic dynamical systems which are "hyperbolic," i.e. which are strongly chaotic: see refs. 27 and 28. It is expected that the deterministic Navier–Stokes system has similar behavior as the chaotic systems in those works, e.g. it will have a strange attractor for which there is a finite density of positive Lyapunov exponents. It is therefore reasonable to expect that the refined-ergodic, or large-deviations, hypothesis shall be also valid for Navier–Stokes turbulence. We may note that similar results hold in other areas of physics. For example, in equilibrium statistical mechanics a similar large-deviations property holds for *volume-averages*. The hypothesis there is known as "Boltzmann's principle" and in that case the thermodynamic entropy function S plays the role of $-V$ above. For this reason the large-deviations theory in chaotic dynamical systems by analogy often goes under the name of *thermodynamic formalism*. The large-deviations hypothesis for Navier–Stokes turbulence has, in fact, been independently suggested before from such considerations by Frisch (see Section 4.4 of ref. 25). It is a hypothesis, in any case, which is subject to experimental verification, as discussed further below. We expect it generally to be true.

The function $V[\mathbf{w}]$ which appears in the refined ergodic hypothesis has been called by us the *effective potential*. This terminology is borrowed from quantum field-theory (see refs. 10 and 11). In field-theory it is usually introduced as the time-extensive limit of a so-called *effective action*, which is a functional Γ on time-histories of the variable $\mathbf{W}$. That is,

$$V[\mathbf{w}] = \lim_{T \to \infty} \frac{1}{T} \Gamma[\mathbf{w}_T] \tag{8}$$

in which Γ is the effective action and $\mathbf{w}_T$ is the time-extended history

$$\mathbf{w}_T(t) \equiv \begin{cases} \mathbf{w} & \text{if } 0 < t < T \\ \bar{\mathbf{w}} & \text{otherwise} \end{cases} \tag{9}$$

In probabilistic large-deviations theory V is usually called the *rate function* or *entropy function*. For deterministic dynamical systems it is very simply related to the Kolmogorov–Sinai or dynamical entropy (see refs. 27 and 28). Mandelbrot[29] has proposed that it be called the *Cramér function*. We shall employ here the terminology already in use in quantum field-theory. Note

that the most important properties of V follow readily from the Eq. (8). As shown in refs. 10 and 11, it satisfies

$$\text{(i)} \quad (\textit{positivity}) \qquad V[\mathbf{w}] \geqslant 0 \tag{10}$$

$$\text{(ii)} \quad (\textit{unique minimum}) \qquad V[\mathbf{w}] = 0 \quad \text{iff} \quad \mathbf{w} = \bar{\mathbf{w}} \tag{11}$$

$$\text{(iii)} \quad (\textit{convexity}) \qquad \lambda V[\mathbf{w}] + (1-\lambda)\, V[\mathbf{w}'] \geqslant V[\lambda \mathbf{w} + (1-\lambda)\, \mathbf{w}'], \qquad 0 < \lambda < 1 \tag{12}$$

Of course, the condition of positivity is obvious, for a negative V would imply probabilities >1. The condition of unique minimum might be violated if there were "ergodicity-breaking" associated to multiple coexisting attractors of the dynamics. This would be similar to the existence of multiple Gibbs states and the occurrence of phase-transitions in equilibrium statistical mechanics. However, while it might happen at some intermediate Reynolds numbers subsequent to the first instability, it is very unlikely to occur in the fully-developed turbulent regime at high Reynolds number. The last condition of convexity arises from Hölder realizability inequalities (see refs. 10 and 11). Observe that V has units of 1/(time) and that $(V(\mathbf{w}))^{-1}$ represents the averaging-time necessary to reduce e-fold the probability of the fluctuation value $\mathbf{w}$.

As discussed previously,[17] it is possible to measure the effective potential for any variable $\mathbf{W}$ (which ought, properly, to be written with a subscript as $V_{\mathbf{W}}$ to indicate the variable(s) considered). This requires only having a long time-series $\mathbf{W}(t)$ of the variable in question, which could be obtained either from experiment or from DNS. See ref. 17 for details. Note, in particular, that such a measurement would empirically verify the refined ergodic hypothesis. It would be very useful to determine the potentials of interesting turbulence statistics both from experiment and simulation. Although less traditional, the effective potentials are at least equally important statistical characteristics of the turbulence as, say, Fourier spectra. Also, as we discuss next, they are theoretically accessible within an important class of closures.

2.2. PDF-Based Moment-Closures and the Rayleigh–Ritz Method

Moment-closures may be described in general terms as follows: given a dynamical system governed by differential equations $\dot{\mathbf{x}} = \mathbf{K}(\mathbf{x})$ one defines a *Liouville operator* $\hat{L}$ as

$$\hat{L} = -\sum_i \frac{\partial}{\partial x_i} (K_i(\mathbf{x}) \cdot) \tag{13}$$

This operator governs the evolution of the PDF of the system via the Liouville equation

$$\partial_t P(\mathbf{x}, t) = \hat{L} P(\mathbf{x}, t) \tag{14}$$

In general, one may be interested in some finite set of *moments* of the PDF,

$$\boldsymbol{\mu}(t) \equiv \langle \boldsymbol{\psi} \rangle_t = \int d\mathbf{x}\, \boldsymbol{\psi}(\mathbf{x})\, P(\mathbf{x}, t) \tag{15}$$

where $\boldsymbol{\psi}(\mathbf{x}) = (\psi_1(\mathbf{x}),..., \psi_S(\mathbf{x}))$ is a selected set of functions. Equations for the moments follow directly from Eq. (14), as

$$\dot{\boldsymbol{\mu}}(t) = \langle \hat{L}^\dagger \boldsymbol{\psi} \rangle_t \tag{16}$$

where $\hat{L}^\dagger = \sum_i K_i(\mathbf{x})\, \partial/\partial x_i$ is the adjoint of the Liouville operator. The basic difficulty is that for a nonlinear dynamics the average on the righthand side of Eq. (16) is not a function of the given moments $\boldsymbol{\mu}(t)$ themselves, but also involves additional higher-order moments. This is just the general *closure problem* of nonequilibrium statistical dynamics. A standard procedure to handle the difficulty in a pragmatic fashion is to make *ad hoc* "closures" for the unknown terms involving the higher-moments, by which they are represented in terms of the retained moments $\boldsymbol{\mu}(t)$. In this way a closed dynamical equation

$$\dot{\boldsymbol{\mu}}(t) = \mathbf{V}(\boldsymbol{\mu}(t)) \tag{17}$$

is obtained for those moments which may then be solved by standard numerical methods.

A somewhat more systematic approach to the problem is to make a model for the actual statistical distribution $P(\cdot, t)$ at time t. In other words, one may attempt to guess a functional form for P, based upon one's physical insight, past experience, or some empirical information. Often, rather than an explicit PDF function, one will instead propose some surrogate variables $\mathbf{X}$ with specified distributions which are supposed to model the actual realizations of the system. In general, the model PDF's or *surrogate variables* are selected so that they are fully determined once the moments $\boldsymbol{\mu}(t)$ are given (although in principle they may be determined as well by the full set of moments $\{\boldsymbol{\mu}(t'): t' \leqslant t\}$ at all past times). In that case, a closed moment equation is obtained as above with

$$\mathbf{V}(\boldsymbol{\mu}) = \langle \hat{L}^\dagger \boldsymbol{\psi} \rangle_{\boldsymbol{\mu}} \tag{18}$$

where $\langle \cdot \rangle_{\boldsymbol{\mu}}$ denotes the average over the model PDF or surrogate variables specified by the moment-values $\boldsymbol{\mu}$. This is the method of *PDF-based moment closure*, and it is essentially the idea used in refs. 12–16. Observe that this method of moment-closure yields far more information than simple modeling of the moment hierarchy equations. Now a solution $\boldsymbol{\mu}_*(t)$ of the moment equation Eq. (17) yields a plausible guess $P_*(\mathbf{x}, t) = P(\mathbf{x}, \boldsymbol{\mu}_*(t))$ for the entire PDF. Therefore, predictions for any desired statistical average may be obtained and not merely for the averages of the original functions $\boldsymbol{\psi}$. A variation of the PDF method as outlined above is to parametrize the PDF or the distribution of the surrogates $\mathbf{X}$ by some set of variables $\boldsymbol{\beta}$ other than the moments $\boldsymbol{\mu}$ themselves. These two formulations are equivalent as long as $\boldsymbol{\beta}$ and $\boldsymbol{\mu}$ uniquely determine each other. An infinite-dimensional version of this scheme is the mapping closure for passive scalars [12], in which the amplitude mapping function $X(\theta_0, t)$ corresponds to $\boldsymbol{\beta}$ and the set of moment functions are just $\psi_n[\theta] = [\theta(x)]^n$, $n = 0, 1, 2, \ldots$, or, equivalently, arbitrary functions $\boldsymbol{\Psi}(\theta(x))$ of the scalar field $\theta(x)$ at a single space-point x.

As explained in ref. 11, it is possible to give the PDF closure a *variational formulation*, analogous to the Rayleigh–Ritz characterization of wave-functions in quantum theory. Let us consider here only the formulation for the stationary state. In that case, the moment equations become just some nonlinear equations

$$\mathbf{V}(\boldsymbol{\mu}) = \mathbf{0} \tag{19}$$

whose roots $\boldsymbol{\mu}_*$ are the predicted values for the moments in the statistical stationary-state of the system. Now, an equivalent formulation as Eq. (19) is the following: Let

$$\boldsymbol{\Psi}^R(\mathbf{x}, \bar{\boldsymbol{\mu}}) \equiv \mu_0 P(\mathbf{x}; \boldsymbol{\mu}) \tag{20}$$

where $\bar{\boldsymbol{\mu}} = (\mu_0, \boldsymbol{\mu})$ and

$$\boldsymbol{\Psi}^L(\mathbf{x}; \bar{\boldsymbol{\alpha}}) \equiv \sum_{i=0}^{S} \alpha_i \psi_i(\mathbf{x}) \tag{21}$$

with $\bar{\alpha} = (\alpha_0, \boldsymbol{\alpha})$ and $\psi_0(\mathbf{x}) \equiv 1$. In other words, $\boldsymbol{\Psi}^R$ is the PDF *Ansatz* itself but with an arbitrary normalization factor μ_0. On the other hand, $\boldsymbol{\Psi}^L$ is an arbitrary linear superposition of the moment functions $\psi_i(\mathbf{x})$, including the constant or zeroeth-order moment function $\psi_0(\mathbf{x}) \equiv 1$. Now it is easy to

check that *the solutions of the moment equation Eq.* (19) *are characterized equivalently as the stationary points* $(\bar{\boldsymbol{\alpha}}_*, \bar{\boldsymbol{\mu}}_*)$ *of the "Hamiltonian"*

$$\mathscr{H}(\bar{\boldsymbol{\alpha}}, \bar{\boldsymbol{\mu}}) \equiv -\int d\mathbf{x}\, \boldsymbol{\Psi}^L(\mathbf{x}; \bar{\boldsymbol{\alpha}})^* \cdot \hat{L}\boldsymbol{\Psi}^R(\mathbf{x}; \bar{\boldsymbol{\mu}}) \tag{22}$$

under arbitrary variations of $\bar{\boldsymbol{\alpha}}$, $\bar{\boldsymbol{\mu}}$ *such that* $\bar{\boldsymbol{\alpha}}_* = (1, 0)$. In fact, the stationarity equations under the variation of $\bar{\boldsymbol{\alpha}}$ are just Eq. (19), while the stationarity equations under the variation of $\bar{\boldsymbol{\mu}}$ reduce to the conservation of normalization condition

$$\int d\mathbf{x}\, \hat{L}P(\mathbf{x}; \boldsymbol{\mu}_*) = 0 \tag{23}$$

when $\bar{\boldsymbol{\alpha}}_* = (1, \mathbf{0})$. Observe that if the "Hamiltonian" $\mathscr{H}[\boldsymbol{\Psi}^R, \boldsymbol{\Psi}^L] = -\int d\mathbf{x}\, \boldsymbol{\Psi}^L(\mathbf{x}) \cdot \hat{L}\boldsymbol{\Psi}^R(\mathbf{x})$ were varied over all possible $\boldsymbol{\Psi}^R$, $\boldsymbol{\Psi}^L$, then one would recover the *exact* equations

$$\hat{L}\boldsymbol{\Psi}^R = 0 \qquad \text{and} \qquad \hat{L}^\dagger \boldsymbol{\Psi}^L = 0 \tag{24}$$

whose solutions are $\boldsymbol{\Psi}^R(\mathbf{x}) = P_s(\mathbf{x})$, the true stationary PDF, and $\boldsymbol{\Psi}^L(\mathbf{x}) \equiv 1$. The previous approximate solution of the Eqs. (24) is just an example of the numerical "method of weighted residuals," which is well-known to have a variational formulation for non-self-adjoint problems in terms of the equation and its adjoint (see Chapter 9 of ref. 30).

The advantage of this variational formulation is that it yields also a simple Rayleigh–Ritz method to approximate the effective potentials of the system. In refs. 10 and 11 it was shown that the effective potential $V = V_{\mathbf{w}}$ has the following variational characterization: $V[\mathbf{w}]$ *is equal to the value of the "Hamiltonian"* $\mathscr{H}[\boldsymbol{\Psi}^R, \boldsymbol{\Psi}^L] = -\langle \boldsymbol{\Psi}^L, \hat{L}\boldsymbol{\Psi}^R \rangle$ *at the stationary point, when that is varied over all trial functions* $\boldsymbol{\Psi}^R$, $\boldsymbol{\Psi}^L$ *subject to the constraints*

$$\langle \boldsymbol{\Psi}^L, \hat{\mathbf{W}}\boldsymbol{\Psi}^R \rangle = \mathbf{w} \tag{25}$$

and

$$\langle \boldsymbol{\Psi}^L, \boldsymbol{\Psi}^R \rangle = 1 \tag{26}$$

Observe that $\langle \boldsymbol{\Psi}^L, \boldsymbol{\Psi}^R \rangle = \int d\mathbf{x}\, \boldsymbol{\Psi}^L(\mathbf{x})^*\, \boldsymbol{\Psi}^R(\mathbf{x})$ and that $\hat{\mathbf{W}}$ represents the operator of multiplication by the variable $\mathbf{W}(\mathbf{x})$. Using the same *Ansätze* for $\boldsymbol{\Psi}^R$ and $\boldsymbol{\Psi}^L$ as within the variational formulation of PDF closure above, one obtains a simple algorithm to approximate V. It may be described succinctly as follows (for further details, see refs. 11 and 31):

The constraints in Eqs. (25)–(26) may be incorporated by suitable Lagrange multipliers $\mathbf{h}$ and λ, respectively. Define $(S+1)$-dimensional vectors $\bar{\mathbf{m}} = \mu_0(1, \boldsymbol{\mu})$ and also $\bar{\mathbf{V}}(\bar{\boldsymbol{\mu}}, \mathbf{h}) = \mu_0(V_0(\boldsymbol{\mu}, \mathbf{h}), \mathbf{V}(\boldsymbol{\mu}, \mathbf{h}))$ by

$$\bar{V}_i(\bar{\boldsymbol{\mu}}, \mathbf{h}) = \langle (\hat{L} + \mathbf{h} \cdot \hat{\mathbf{W}})^\dagger \psi_i \rangle_{\bar{\boldsymbol{\mu}}} \tag{27}$$

for $i = 0, 1, \ldots, S$, where $\langle \cdot \rangle_{\bar{\boldsymbol{\mu}}}$ denotes average with respect to $\boldsymbol{\Psi}^R$ in Eq. (20). Next, let

$$\mathbf{B}(\bar{\boldsymbol{\mu}}) \equiv \frac{\partial \bar{\mathbf{m}}}{\partial \bar{\boldsymbol{\mu}}} = \begin{pmatrix} 1 & \boldsymbol{\mu} \\ \mathbf{0} & \mu_0 \mathbf{1} \end{pmatrix} \tag{28}$$

and

$$\mathbf{A}(\bar{\boldsymbol{\mu}}, \mathbf{h}) \equiv \frac{\partial \bar{\mathbf{V}}}{\partial \bar{\boldsymbol{\mu}}}(\bar{\boldsymbol{\mu}}, \mathbf{h}) = \begin{pmatrix} V_0(\boldsymbol{\mu}, \mathbf{h}) & \mathbf{V}(\boldsymbol{\mu}, \mathbf{h}) \\ \mu_0 \dfrac{\partial V_0}{\partial \boldsymbol{\mu}}(\boldsymbol{\mu}, \mathbf{h}) & \mu_0 \dfrac{\partial \mathbf{V}}{\partial \boldsymbol{\mu}}(\boldsymbol{\mu}, \mathbf{h}) \end{pmatrix} \tag{29}$$

Then, within the *Ansatz* considered for $\boldsymbol{\Psi}^R$, $\boldsymbol{\Psi}^L$, Eqs. (20)–(21), it follows that for each $\mathbf{h}$, the following equations must be simultaneously solved:

$$\mathbf{A}(\bar{\boldsymbol{\mu}}, \mathbf{h}) \cdot \bar{\boldsymbol{\alpha}} = \lambda \mathbf{B}(\bar{\boldsymbol{\mu}}) \cdot \bar{\boldsymbol{\alpha}} \tag{30}$$

$$\mathbf{V}(\boldsymbol{\mu}, \mathbf{h}) = \lambda \boldsymbol{\mu} \tag{31}$$

$$\alpha_0 + \sum_{i=1}^{S} \alpha_i \mu_i = 1 \tag{32}$$

Observe that μ_0 drops out of this system, and may be set to $\mu_0 = 1$. However, values $\bar{\boldsymbol{\alpha}}_*(\mathbf{h})$, $\mathbf{m}_*(\mathbf{h})$, $\lambda_*(\mathbf{h})$ will be determined for the other variables at each value of $\mathbf{h}$. It is not hard to show that a solution will exist to these equations at least for small $|\mathbf{h}|$, whenever the stability matrix $\mathbf{J} = (\partial \mathbf{V}/\partial \boldsymbol{\mu})^\perp(\boldsymbol{\mu}_*)$ of the dynamical vector field $\mathbf{V}(\boldsymbol{\mu})$ is nonsingular at the fixed point $\boldsymbol{\mu}_*$ (see ref. 31). In that case, the approximation to the effective potential V is given as

$$\begin{aligned} V_*(\mathbf{h}) &= -\langle \boldsymbol{\Psi}^L(\bar{\boldsymbol{\alpha}}_*(\mathbf{h})), \hat{L} \boldsymbol{\Psi}^R(\bar{\boldsymbol{\mu}}_*(\mathbf{h})) \rangle \\ &= -\sum_{i=1}^{S} \alpha_{*i}(\mathbf{h})\, V_i(\boldsymbol{\mu}_*(\mathbf{h})) \end{aligned} \tag{33}$$

The second sum is taken with index i starting at $i=1$, since the $i=0$ term vanishes identically. Of course, one really wishes to have V_* as a function of $\mathbf{w}$. For that purpose, one must calculate

$$\mathbf{w}_*(\mathbf{h}) = \langle \Psi^L(\bar{\alpha}_*(\mathbf{h})), \hat{\mathbf{W}}\Psi^R(\bar{\mu}_*(\mathbf{h}))\rangle \tag{34}$$

Inverting $\mathbf{w}_*(\mathbf{h})$ to find the function $\mathbf{h}_*(\mathbf{w})$, one then obtains

$$V_*(\mathbf{w}) = V_*(\mathbf{h}_*(\mathbf{w})) \tag{35}$$

This is the final Rayleigh–Ritz approximation to the effective potential within a PDF *Ansatz*.

Let us now make several important observations concerning the Rayleigh–Ritz approximation procedure for the effective potential V. In principle, any fixed point $\boldsymbol{\mu}_*$ of the closure dynamical vector $\mathbf{V}(\boldsymbol{\mu})$ may be taken as the starting point of the calculation. Indeed, it is easy to check that the Eqs. (30)–(32) are then satisfied at $\mathbf{h}=\mathbf{0}$ by $(\alpha_0, \boldsymbol{\alpha}, \boldsymbol{\mu}, \lambda) = (1, \mathbf{0}, \boldsymbol{\mu}_*, 0)$. However the method should, in fact, only be applied if $\boldsymbol{\mu}_*$ is a *stable* fixed point of $\mathbf{V}(\boldsymbol{\mu})$. The reason is that, as discussed in refs. 10 and 11, the quantity $\lambda_*(\mathbf{h})$ should correspond to the *principal eigenvalue* of the "perturbed" Liouville operator $\hat{L} + \mathbf{h}\cdot\hat{\mathbf{W}}$, or, in other words, the eigenvalue with the largest real part. For the full infinite-dimensional operator it is known that this eigenvalue corresponds to the "zero-branch" $\lambda(\mathbf{0})=0$, i.e. the branch which passes through 0 at $\mathbf{h}=\mathbf{0}$. However, in the approximation considered the zero-branch of eigenvalues only coincides with the branch of principal eigenvalues if the fixed point $\boldsymbol{\mu}_*$ is linearly stable. For that reason, *consistency requires that only stable fixed points of the closure equations be considered.* Next, we note that to calculate one point of the graph of $V_*[\mathbf{w}]$ vs. $\mathbf{w}$ requires to solve the coupled Eqs. (30)–(32) for precisely one value of $\mathbf{h}(=\mathbf{h}_*[\mathbf{w}])$. This is a problem of determining fixed points of the same type as that of finding fixed points of the original closure dynamics, c.f. Eq. (19). Indeed, given a fixed point $\boldsymbol{\mu}_*$ of the closure equation, one automatically has a joint fixed point of the Eqs. (30)–(32) for $\mathbf{h}=\mathbf{0}$. Therefore, it is not hard to track a succession of roots for some values of $\mathbf{h}$ in the neighborhood of $\mathbf{h}=\mathbf{0}$. *Thus, the computational expense to calculate the effective potential in the neighborhood of the predicted closure mean is of the same order as to calculate the mean value itself.* Lastly, we note that the Rayleigh–Ritz calculation makes essential use of the actual dynamics, through the Liouville operator. It further exercises the PDF *Ansatz*, Eq. (20), as well, since it requires additional moments $\langle W_\alpha \psi_i\rangle_{\boldsymbol{\mu}}$ not appearing in the original closure equations. Thus, *the Rayleigh–Ritz potential contains more information both from the microscopic dynamics and from*

the PDF Ansatz *than is contained in the original closure equations themselves.* Note that this is true even if the variable **W** corresponds to one of the moment-functions ψ_i used in constructing the closure.

The Rayleigh–Ritz construction guarantees that the approximate potential $V_*[\mathbf{w}]$ enjoys many of the same properties as the true potential $V(\mathbf{w})$. It may be shown that

$$V_*(\mathbf{w}) = \mathbf{h} \cdot \mathbf{w}_*(\mathbf{h}) - \lambda_*(\mathbf{h}) \tag{36}$$

and that

$$\frac{\partial \lambda_*}{\partial \mathbf{h}}(\mathbf{h}) = \mathbf{w}_*(\mathbf{h}) \tag{37}$$

where $\mathbf{w}_*(\mathbf{h})$ is the function defined in Eq. (34). The latter equation is analogous to the *Hellmann–Feynman theorem* in quantum-mechanical perturbation theory, while the former states that $V_*(\mathbf{w})$ is the *Legendre transform* of $\lambda_*(\mathbf{h})$. (The proofs in ref. 11 do not apply to the *Ansatz* Eqs. (20)–(21), but it may nonetheless be shown that these facts still hold: see ref. 31.) It is a consequence that the property (ii) of the exact potential holds also for the Rayleigh–Ritz potential:

$$V_*[\bar{\mathbf{w}}_*] = 0 \qquad \text{and} \qquad \frac{\partial V_*}{\partial \mathbf{w}}[\bar{\mathbf{w}}_*] = \mathbf{0} \tag{38}$$

Here $\bar{\mathbf{w}}_* = \langle \mathbf{W} \rangle_{\boldsymbol{\mu}_*}$ is the average of **W** in the *Ansatz* at the fixed point value $\boldsymbol{\mu}_*$. Thus, the closure mean is a zero and also a critical point of V_*. However, neither property (i), positivity, nor property (iii), convexity, are guaranteed to hold for the Rayleigh–Ritz potential.

2.3. Practical Applications of the Theory

Using the above analytical results we may now justify the following applied principles:

Realizability Criterion. *A closure predicted mean value* $\bar{\mathbf{w}}_* = \langle \mathbf{W} \rangle_{\boldsymbol{\mu}_*}$ *for which the corresponding approximate potential* $V_*(\mathbf{w})$ *does not satisfy all realizability conditions* (i)–(iii) *must be rejected.* In ref. 17 it was shown that the Rayleigh–Ritz approximation converges to the true potential as the PDF *Ansatz* is successively improved. See also below. Furthermore, this convergence is (in all cases observed) from the mean value

outward. Thus, a failure of realizability in the neighborhood of the predicted mean implies that convergence has not yet occurred even locally. In particular, the mean value is not yet converged and its predicted value cannot be trusted. Put another way, if the closure does not describe correctly the small fluctuations of $\mathbf{W}$ near its predicted mean, then it is unlikely to describe correctly the mean value itself. This is particularly likely in strongly noisy systems such as turbulent flows, in which the fluctuations make an important contribution to the means. Clearly, these arguments are not rigorous, but only plausible. Below we shall check in concrete examples the validity of the criterion.

Optimization Principle. *If the* PDF Ansatz *contains a free parameter c then the optimum value of that parameter to predict the average $\bar{\mathbf{w}}_* = \langle \mathbf{W} \rangle_{\mu_*}$ is the value c_* for which the approximate potential $V_*(\mathbf{w}; c)$ is stationary under variations of c (if such a value exists).* This principle can be motivated on the basis of the variational characterization of the effective potential, which expresses $V[\mathbf{w}]$ as the value of the "Hamiltonian" at a stationary point under all variations with the constraint of fixed $\mathbf{w}$. This gives the principle an analytical basis, but there are also intuitive considerations in favor of it. If a PDF *Ansatz* is "converged" for a particular mean statistic (in the sense that the calculated mean changes only within a specified tolerance under further refinement of the *Ansatz*), then the result should not depend upon any arbitrary parameter in the model PDF. To the extent that such dependence exists, it indicates a failure of the *Ansatz* to be converged for that variable. It is thus reasonable to select as the "best" value of the arbitrary parameter that at which the dependence is the smallest. The optimization principle that is proposed thus corresponds to a *principle of minimal sensitivity*[32] of the predicted mean to any free parameters in the PDF *Ansatz*. However, there are important caveats:

First, for a given value of $\mathbf{w}$ there may be more than one stationary point. The phenomenon occurs in practice within PDF closures, as discussed in Appendix II. This leaves some ambiguity as to which stationary point to consider in making an approximation. It is shown in Appendix II that, for *any* value of $\mathbf{w}$ obtained as the average $\langle \mathbf{W} \rangle_{\mu_*(c)}$ for *some* value of the free parameter $c = c_0$, $V_*(\mathbf{w}; c)$ is stationary under variations of c at the point $c = c_0$ itself. However, choosing this as the stationary point for such $\mathbf{w}$ values would make the resulting approximate potential vanish at all such points in $\mathbf{w}$-space. This would lead to an approximate potential which vanished at many points, violating the ergodic hypothesis. In addition to this unphysical feature of the approximation, the "optimum" value of c selected would then depend upon the point $\mathbf{w}$ considered. It is shown in Appendix II that, in order to have *one* value $c = c_*$ be a stationary point

of $V_*(\mathbf{w}; c)$ for *all* $\mathbf{w}$, it is necessary, in particular, that the average $\bar{\mathbf{w}}(c) = \langle \mathbf{W} \rangle_{\mu_*(c)}$ be stationary at the same value, i.e. c_* must be a critical point of $\bar{\mathbf{w}}(c)$. This is a strong constraint on the c-values, which will generally select only a few candidates for "optimum" values c_*. It must then be seen whether the potentials themselves are stationary as well.[3] It cannot be said in advance how successful such an optimization principle will be. We shall examine below how well it succeeds in concrete closures for the 3-mode system. Unlike the closely analogous Rayleigh–Ritz methods used in quantum theory, the present principle does not yield *bounds* for the approximated potential. This is a consequence of the non-self-adjointness of the evolution operator $\hat{L}$ for dissipative dynamics. In quantum mechanics with self-adjoint Hamiltonian operator the corresponding characterization of the potential is via a constrained *minimization* of the expected energy value. Hence, the approximating potential is always an upper bound and, furthermore, must approach the exact answer monotonically as more parameters are added to the trial *Ansatz*. In the present case, adding parameters may even lead temporarily to a *worse* approximation. It is only guaranteed to converge sufficiently closely when a large enough number of parameters are added to the *Ansatz*.[4]

Nevertheless, we believe that the methods proposed here are the closest analogue conceivable to the Rayleigh–Ritz methods already extensively utilized in quantum many-body theory and field-theory. We believe that our similar approach will be very fruitful in turbulence and also in other problems of nonequilibrium statistical dynamics with strong nonlinearity. It allows intuitive PDF *Ansätze* or guesses of the turbulence statistics to be incorporated into analytical calculations, using the exact equations of motion of the system. The variational method then yields useful direct checks on the physical ideas motivating the PDF *Ansätze* employed. Granted that no systematic derivation of closure approximations is possible, this seems to us a rational alternative.

[3] In practice, however, it may be difficult to detect a non-stationarity of $V_*(\mathbf{w}; c)$ at values $\mathbf{w}$ far from the mean value $\bar{\mathbf{w}}(c_*)$. Any critical point c_* of $\bar{\mathbf{w}}(c)$ will *appear* to be a stationary point of $V_*(\mathbf{w}; c)$ at values of $\mathbf{w}$ close enough to the minimum point $\bar{\mathbf{w}}(c_*)$.

[4] It may be of interest in this connection to note that the Donsker-Varadhan theory[26] provides a *minimax characterization* of the effective potential, which sharpens the variational formulation given above. In fact, if one makes the change of variables $\Psi_L = u$ and $\Psi_R = P/u$, with P a normalized PDF and with $u > 0$, then it is proved[26] that

$$V[\mathbf{w}] = \inf_{\{P : \int \mathbf{W}\, dP = \mathbf{w}\}} \sup_{u>0} \left[-\int \frac{\hat{L}^\dagger u}{u}\, dP \right] \tag{39}$$

With this choice of variables the stationary point is seen to be always of saddle-type.

3. FIRST EXAMPLE: HERMITE-EXPANSION PDF ANSATZ

Our first example of the variational method will be with a PDF *Ansatz* based upon expansion in Hermite polynomials orthogonal on a trial Gaussian weight. This representation of turbulence distributions was apparently first suggested by Hopf and subsequently worked out in some detail by Edwards.[33] It is very similar to representations of 1-particle distributions used in the kinetic theory of gases, such as the Chapman–Enskog solution of the Boltzmann equation. The analogous expansion of Boltzmann solutions in terms of Hermite polynomials was already used in the middle of this century by Grad.[34] These representations have one defect, which is that the resulting distributions are not everywhere positive, but become negative at some points. This failure of realizability for the Hermite-expansion distributions need not be fatal, as the negative values in the kinetic theory problem occur at extremely high velocities. Indeed, the Navier–Stokes equations emerge from such unrealizable distributions in the first-order Chapman–Enskog solutions of the Boltzmann equation, yet Navier–Stokes equations are certainly very useful!

These problems may be expected to be more serious for turbulence, since there is no scale-separation and the negative values of PDF's are likely to occur much closer to the physically significant set of realizations. Perhaps a more serious defect limiting the usefulness of systematic Hermite expansions is the large number of degrees-of-freedom involved. The number of Fourier modes that must be minimally retained for a developed turbulent flow grows as $\mathcal{N} \sim (Re)^{9/4}$, in terms of the Reynolds number Re. However, the number of Hermite polynomials of degree D grows even faster, $\sim \mathcal{N}^D$! While the 3-mode dynamics we consider here is simple enough that convergence can often be obtained, it is clearly unfeasible to include many terms in a systematic Hermite polynomial expansion of PDF's for Navier–Stokes turbulence. However, there may still be some limited usefulness of low-order Hermite expansions in that case. It is shown elsewhere[35] that second-order Reynolds-stress closures may be obtained from cubic order Hermite-expansion PDF's in the case of homogeneous turbulence.

In any case, we shall examine these Hermite-expansion PDF models here as one example of the application of the variational methods. The PDF *Ansatz* is as follows:

$$P(\mathbf{x}; \beta, \boldsymbol{\sigma}) = w(\mathbf{x}; \boldsymbol{\sigma}) \times \sum_{\mathbf{n}=\mathbf{0}}^{N} \beta_{\mathbf{n}} \frac{He_{\mathbf{n}}(\mathbf{x}; \boldsymbol{\sigma})}{\sqrt{\mathbf{n}!}} \tag{40}$$

where $\boldsymbol{\sigma} = (\sigma_1, \sigma_2, \sigma_3)$, $\mathbf{n} = (n_1, n_2, n_3)$, $\mathbf{N} = (N_1, N_2, N_3)$,

$$w(\mathbf{x}; \boldsymbol{\sigma}) = \frac{1}{\sqrt{(2\pi)^3 \sigma_1^2 \sigma_2^2 \sigma_3^2}} \exp\left[-\left(\frac{x_1^2}{2\sigma_1^2} + \frac{x_2^2}{2\sigma_2^2} + \frac{x_3^2}{2\sigma_3^2} \right) \right] \tag{41}$$

and

$$He_{\mathbf{n}}(\mathbf{x}; \boldsymbol{\sigma}) = He_{n_1}(x_1; \sigma_1)\, He_{n_2}(x_2; \sigma_2)\, He_{n_3}(x_3; \sigma_3) \tag{42}$$

with $\mathbf{n}! = n_1!\, n_2!\, n_3!$ defining the factorial of the multi-index $\mathbf{n}$. The single-variable Hermite polynomials $He_n(x; \sigma)$ are defined for $n = 0, 1, 2, \ldots$ via

$$\frac{(-1)^n \sigma^n}{n!} \frac{d^n}{dx^n} e^{-x^2/2\sigma^2} = He_n(x; \sigma) \cdot e^{-x^2/2\sigma^2} \tag{43}$$

These polynomials have many properties, including orthogonality with respect to the Gaussian weight, and are reviewed, e.g., in ref. 36, Chapter 22. To complete the closure, a specification of the moment-functions is also required. It is most natural to take

$$\psi_{\mathbf{n}}(\mathbf{x}; \boldsymbol{\sigma}) = He_{\mathbf{n}}(\mathbf{x}; \boldsymbol{\sigma}) \tag{44}$$

in which case $\mu_{\mathbf{n}} = \langle \psi_{\mathbf{n}} \rangle = \beta_{\mathbf{n}}$ are the corresponding Hermite-polynomial moments for the PDF-*Ansatz* Eq. (40). The resulting closure equations are *linear* for this case:

$$\dot{\mu}_{\mathbf{n}} = \sum_{\mathbf{m}=\mathbf{0}}^{\mathbf{N}} L(\mathbf{n}; \mathbf{m})\, \mu_{\mathbf{m}} \tag{45}$$

with

$$\begin{aligned} &L(n_1 n_2 n_3; m_1 m_2 m_3) \\ &\quad = A_1 \cdot \frac{\sigma_2 \sigma_3}{\sigma_1} \cdot \sqrt{n_1}\, \delta_{n_1 - 1, m_1} \left[\sqrt{n_2 + 1}\, \delta_{n_2 + 1, m_2} + \sqrt{n_2}\, \delta_{n_2 - 1, m_2} \right] \\ &\qquad \times \left[\sqrt{n_3 + 1}\, \delta_{n_3 + 1, m_3} + \sqrt{n_3}\, \delta_{n_3 - 1, m_3} \right] \\ &\qquad - \nu_1 \left[n_1\, \delta_{n_1, m_1} + \sqrt{n_1(n_1 - 1)}\, \delta_{n_1 - 2, m_1} \right] \cdot \delta_{n_2, m_2}\, \delta_{n_3, m_3} \\ &\qquad + \frac{\kappa_1}{\sigma_1^2} \left[\sqrt{n_1(n_1 - 1)}\, \delta_{n_1 - 2, m_1} \right] \cdot \delta_{n_2, m_2}\, \delta_{n_3, m_3} \\ &\qquad + \text{cyclic permutations } \{1, 2, 3\} \end{aligned} \tag{46}$$

Observe that these equations are just a finite-order Hermite–Galerkin truncation of the original linear Liouville equation and that $\mathbf{L}_{\mathbf{N},\boldsymbol{\sigma}} = (L(\mathbf{n};\mathbf{m}))$ is the matrix approximation of rank $=(N_1+1)(N_2+1)(N_3+1)$ to the infinite-dimensional Liouville operator. In the variational derivation of these equations we take $\Psi^R = P$ in Eq. (40) above, and, likewise,

$$\Psi^L(\mathbf{x};\boldsymbol{\alpha},\boldsymbol{\sigma}) = \sum_{\mathbf{n}=\mathbf{0}}^{\mathbf{N}} \alpha_{\mathbf{n}} \frac{He_{\mathbf{n}}(\mathbf{x};\boldsymbol{\sigma})}{\sqrt{\mathbf{n}!}} \tag{47}$$

There is no need to augment these *Ansätze* by the addition of a constant function, because the zeroeth-order moment is already contained as $He_{\mathbf{0}}(\mathbf{x};\boldsymbol{\sigma}) \equiv 1$. Note that $\mathbf{N}$ and $\boldsymbol{\sigma}$ are *free parameters* of the closure and may be chosen as desired.

(i) Thermal Equilibrium

We shall first consider an equilibrium version of the 3-mode system. As discussed in Appendix 1, the system possesses an absolute-equilibrium, Gaussian stationary distribution whenever $\kappa_i = \Theta\nu_i$ for all $i=1,2,3$ with some fixed Θ. The variance of the stationary distribution is then Θ. As an instance of this type, we consider the choice of system parameters $\kappa_i = 1$, $\nu_i = 1$, $i=1,2,3$. Since all of the modes are equivalent in this case, we take all the *Ansatz* free parameters equal as well: $N_i = N$, $\sigma_i = \sigma$, $i=1,2,3$. We study the resulting closures for various choices of N and σ. For N up to 5, we have found using MATLAB that the matrix $\mathbf{L}_{N,\sigma}$ has a unique zero eigenvalue and that the rest of its spectrum lies in the left half of the complex plane. Thus, the linear closure dynamics for the moments $\boldsymbol{\mu} = (\mu_{\mathbf{n}})$ has a unique, globally stable fixed point $\boldsymbol{\mu}_*$ which determines an approximation $P_*(\mathbf{x};\sigma,N)$ to the stationary measure. The statistics of main interest are now the modal energies $E_i = \frac{1}{2}x_i^2$, whose means are equal for all $i=1,2,3$ (both in the *Ansatz* and in reality). In Fig. 1 we graph the predicted mean energy E for $N=3$ and for a range of σ values. We see that $\sigma=1$ is here a maximum point. Of course, we already know that $\sigma=1$ is the exact value, since $\sigma^2 = \Theta$ and $\Theta = 1$ in the case considered. This is interesting in view of the optimization principle, according to which any potential optimum value of σ must correspond to a critical point of the closure predicted mean value. This motivates us to calculate the effective potentials $V_E(e)$ within the Hermite PDF *Ansatz* for $N=3$ and various values of σ. The results of such a computation are graphed together in Fig. 2. We observe several striking features.

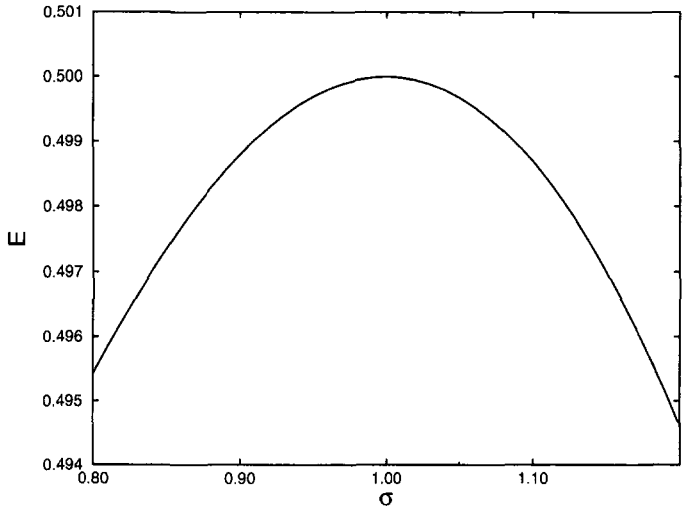

Fig. 1. Mean energy vs. σ in the equilibrium system with $N = 3$ Hermite expansion.

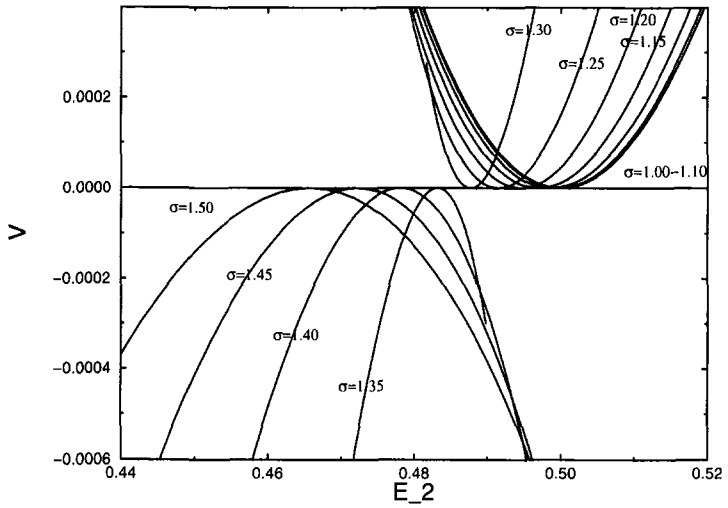

Fig. 2. Effective potential of energy in the equilibrium system with the Hermite expansion, $N = 3$, $\sigma = 1.0$ to 1.5. σ runs in steps of 0.05, moving right to left. The dark line indicates the stationary curve $\sigma = 1.0$.

First, we see that realizability is violated for all $\sigma > 1.3$, although the predicted mean energy in the first such case, $\sigma = 1.35$, is $E = 0.48319554$, disagreeing with the exact result $E = 0.5$ by only 3.4%. This illustrates that the realizability conditions on V_E may be very sensitive tests of the convergence of the closure predictions to the true values. We may test this further by considering higher values of N. For all $N \geqslant 4$ the potentials V_E satisfy realizability in the same range of σ considered above. It is a special feature of the Hermite expansion closure for the equilibrium model that the *exact* result for mean energy $E = 0.5$ is obtained for *all* σ when N is even. Thus, it is not very interesting to consider $N = 4$. However, when $N = 5$ we obtain realizability of the approximate V_E for all $0.5 \leqslant \sigma \leqslant 1.5$. The predicted mean energy for $N = 5$ is the worst when $\sigma = 1.5$, and we graph the corresponding potential in Fig. 3. As noted, realizability is satisfied and, indeed, the predicted mean is $E = 0.49054354$ for $N = 5$, $\sigma = 1.5$, only off by 1.9%. Note, for comparison, that the predicted mean was $E = 0.46579031$ for the instance $N = 3$, $\sigma = 1.5$ in Fig. 2, in which case the prediction was off by 6.8% and realizability of V_E was violated.

However, even more striking is the fact that $\sigma = 1$ is a clear stationary value for the potential $V_E(e)$ under variation of σ. The potentials for $\sigma = 1$ and $\sigma = 1.05$ are essentially indistinguishable, whereas the change is much larger in V_E for other values of σ under the same incremental change. The stationarity at $\sigma = 1$ is verified in further detail in the plot of Fig. 4, which

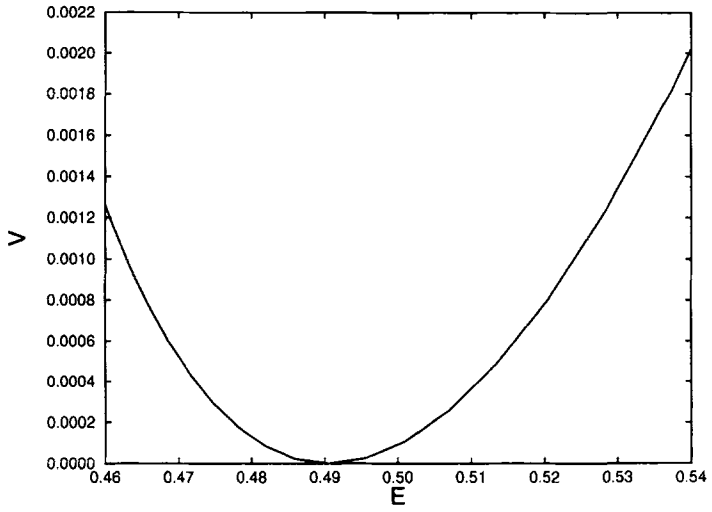

Fig. 3. Effective potential of energy in the equilibrium system with the Hermite expansion, $\sigma = 1.5$, $N = 5$.

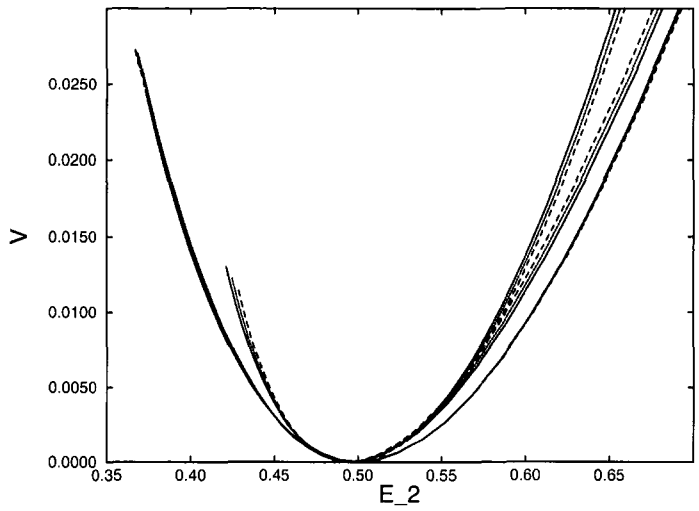

Fig. 4. Comparison of effective potentials under variation of σ. The three groups of curves correspond to $\sigma = 0.80$, 1.00, 1.20 and also each ± 0.01. $\sigma = 1.00$ (heavy solid) is clearly a stationary point.

graphs V_E at $N = 3$ and for $\sigma = 0.8$, 1, and 1.2, as well as nearby values of each. Again, the potential is virtually unchanged at $\sigma = 1$ under the same increment of σ for which the potential changes noticeably near $\sigma = 0.8$ or 1.2. Thus, we see here that the optimization principle selects the *exact* value of σ, and hence also the exact value of mean energy $E = 0.5$.

By taking larger N one should expect a convergence of calculated effective potentials to the true ones. This is one of the advantages in principle of a systematic approximation to PDF's such as Hermite expansions. In Figs. 5 and 6 we plot together the Rayleigh–Ritz approximate potentials V_E from the Hermite expansions in the equilibrium 3-mode system for $\sigma = 1$ and $N = 3$, 4, 5. The plots cover two ranges of E values, the first Fig. 5 with a 10% variation from the mean value and the second Fig. 6 over a larger range with up to 200% variation. We see that in the first interval, the effective potentials for all three N values agree very closely. Hence, the Rayleigh–Ritz approximation here is already converged essentially for $N = 3$. In Fig. 7 the Hermite potentials are compared over this range with those obtained from DNS of the equilibrium 3-mode system, using the method discussed by us previously.[17] The agreement is perfect.

In Fig. 6 we see that $N = 4$ and 5 potentials still agree over the larger range of E, but significant departures are seen from the $N = 3$ potential. Although we do not include the figures, an examination over even a bigger range shows that $N = 4$ and 5 potentials begin to disagree for $E > 2$. This

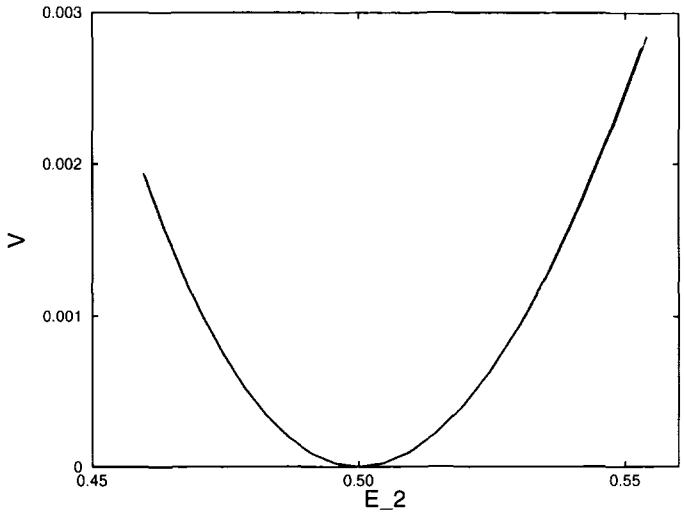

Fig. 5. Effective potential of energy in the equilibrium system with the Hermite expansion, $\sigma = 1$, $N = 3$, 4, 5, $N = 3$ (solid), $N = 4$ (dotted), $N = 5$ (short dash). Over the range shown, the curves are almost indistinguishable.

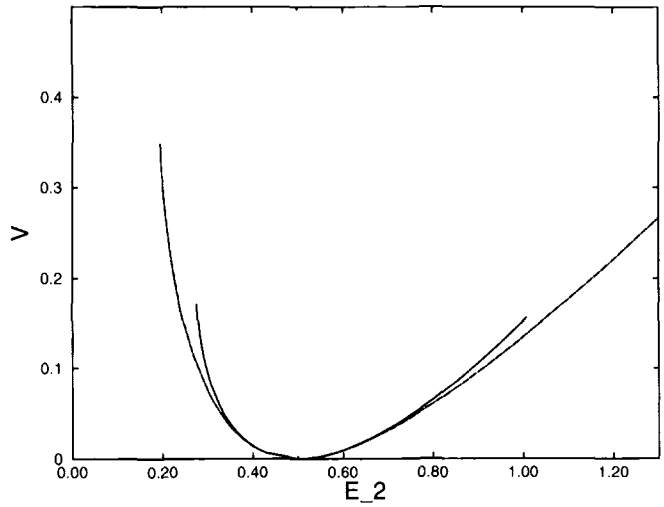

Fig. 6. Effective potential of energy in the equilibrium system with the Hermite expansion, $\sigma = 1$, $N = 3$, 4, 5, $N = 3$ (solid), $N = 4$ (dotted), $N = 5$ (short dash). Over the larger range, only $N = 4$, 5 agree.

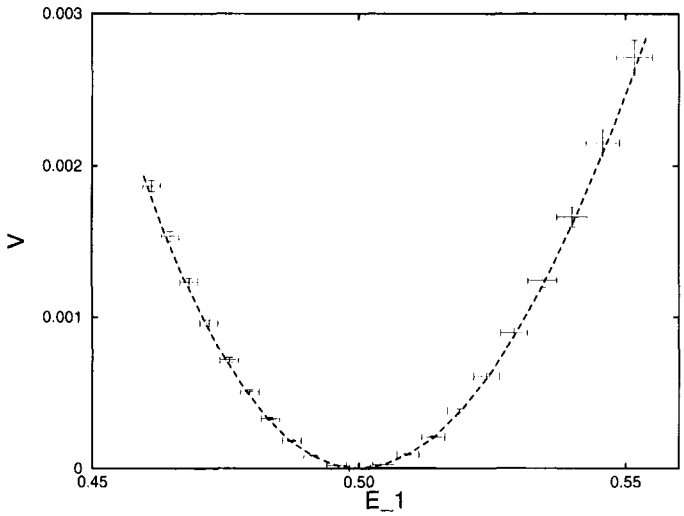

Fig. 7. Effective potential of energy in the equilibrium system with Hermite expansion, $\sigma = 1$, $N = 5$, and with DNS. DNS with errorbars.

example illustrates an important feature that convergence of the effective potentials in the Rayleigh–Ritz approximation scheme is *outward from the minimum*. Of course, this is also as one would expect, since it is more difficult for a PDF *Ansatz* to accurately capture larger fluctuations away from the mean value. However, it is an important consideration in justifying the realizability criterion. If a closure gives an accurate result for the mean of a certain variable, then it should also give a reasonable approximation for fluctuations at least sufficiently close to the mean. For this reason, failure of the effective potential realizability conditions close to the mean imply that the mean value very probably is not converged either. Any agreement with the true mean value must then be a shear accident, and very unlikely in general.

(ii) Dissipative Cascade States

We now turn to the study of cascade states, not in thermal equilibrium. These occur for generic choices of parameter values of the system, other than those satisfying the fluctuation-dissipation relation. Just to be specific, our standard choice in this work is: $A_1 = 2$, $A_2 = A_3 = -1$, $\kappa_1 = 1$, $\kappa_2 = \kappa_3 = 0.001$, $\nu_1 = 0.001$, $\nu_2 = \nu_3 = 1$. As discussed in Appendix 1, the mode-1 then represents a "large-scale" unstable mode which is strongly forced, while modes-2 and 3 represent "small-scale" stable modes which are

strongly damped. An irreversible energy cascade is set up from mode-1 into modes-2 and 3. For each mode of the system a "modal Reynolds number" may be introduced, as:

$$Re_i \equiv \frac{|A_i| X_i'}{\nu_i} \tag{48}$$

with $X_i' = \sqrt{\langle x_i^2 \rangle}$ the rms fluctuation of mode-i. These numbers measure the relative strength of the nonlinear "inertial" terms and the linear damping terms in the dynamics of mode i. It is found from DNS that $X_1' \approx 2.11$, $X_2' = X_3' \approx 0.70$ for the above parameter values, so that $Re_1 \approx 4 \times 10^3$ and $Re_2 = Re_3 \approx 0.7$. Thus, the evolution of mode-1 is dominated by the nonlinear dynamics, while the nonlinear and damping terms play an equally important role in the evolution of modes-2 and 3. The most interesting statistics are the modal energies $E_1 = \frac{1}{2}\langle x_1^2 \rangle$, $E_2 = \frac{1}{2}\langle x_2^2 \rangle$, and the triple correlation $T = \langle x_1 x_2 x_3 \rangle$. It is found from DNS that

$$E_1^{(DNS)} = 2.23 \pm 0.03 \tag{49}$$

$$E_2^{(DNS)} = 0.24939 \pm 0.00001 \tag{50}$$

$$T^{(DNS)} = -0.49777 \pm 0.00003 \tag{51}$$

Notice that the last two values are inferred to the stated high accuracy from the measured value of E_1 and the *exact* equations

$$T = -0.5 + (0.001)\, E_1 \qquad \text{and} \qquad E_2 = 0.5(-T + 0.001) \tag{52}$$

They have also been verified to three digits directly from the DNS. We are interested in predicting these three mean statistics within the Hermite-expansion PDF closures.

Again using MATLAB, we found the matrix approximations $\mathbf{L}_{N,\sigma}$ all have a simple eigenvalue 0 and the rest of the spectrum in the left halfplane. Thus, there is a unique fixed point within the Hermite-expansion *Ansatz* for all σ and $N \leqslant 5$. The mean values of E_1, E_2 and T for $N = 3$ and for values of σ from 5 to 100 are graphed versus σ in Figs. 8–10. In each case, the most noticeable feature is the plateau of values occurring as $\sigma \to \infty$. With superscripts (N, σ) indicating the values of the means for those parameters in the Hermite expansion, we find

$$E_1^{(3,\infty)} = 1.4171 \tag{53}$$

$$E_2^{(3,\infty)} = 0.24979 \tag{54}$$

$$T^{(3,\infty)} = -0.49858 \tag{55}$$

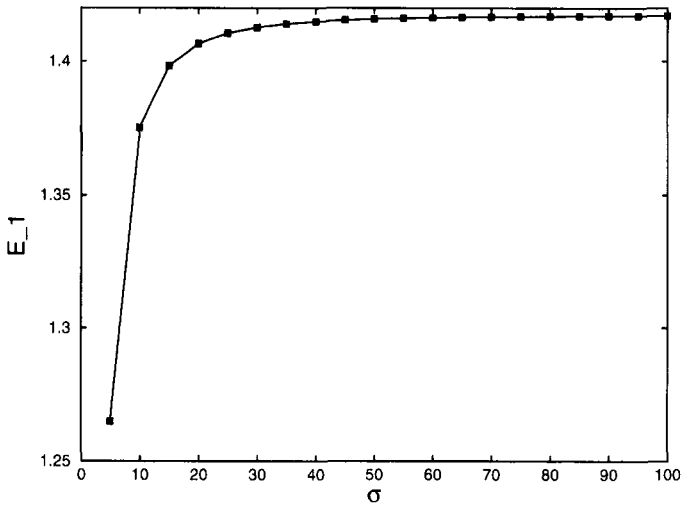

Fig. 8. Mean of E_1 vs. σ in the $N=3$ Hermite expansion for the nonequilibrium system.

These plateau values are of the greatest interest since they are candidates for optimum values, if the corresponding potentials are stationary (approach a limit) as $\sigma \to \infty$. This has been verified to occur, in the somewhat surprising sense that the potentials of all three variables are negative and concave at *every* value of σ and approach the identically zero potential $V \equiv 0$

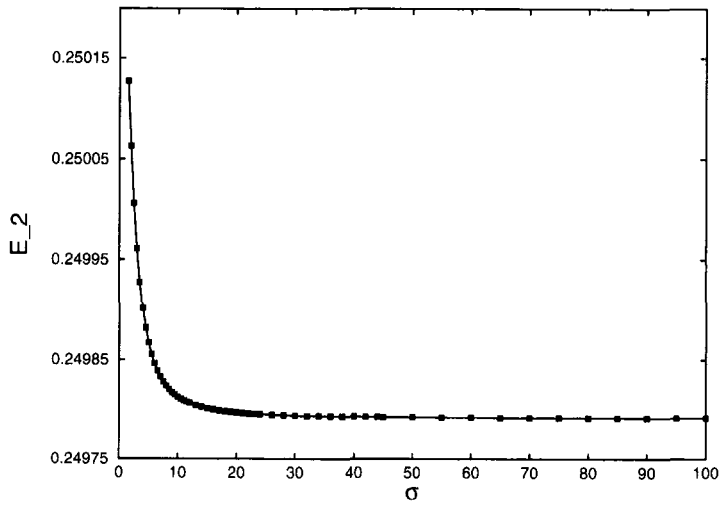

Fig. 9. Mean of E_2 vs. σ in the $N=3$ Hermite expansion for the nonequilibrium system.

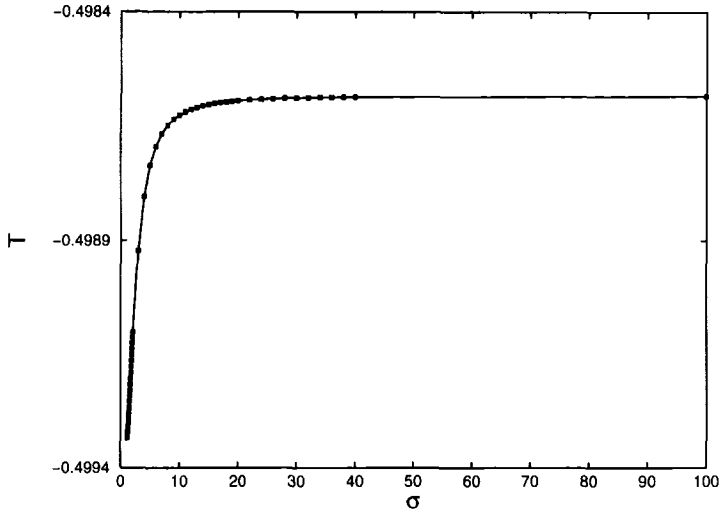

Fig. 10. Mean of T vs. σ in the $N=3$ Hermite expansion for the nonequilibrium system.

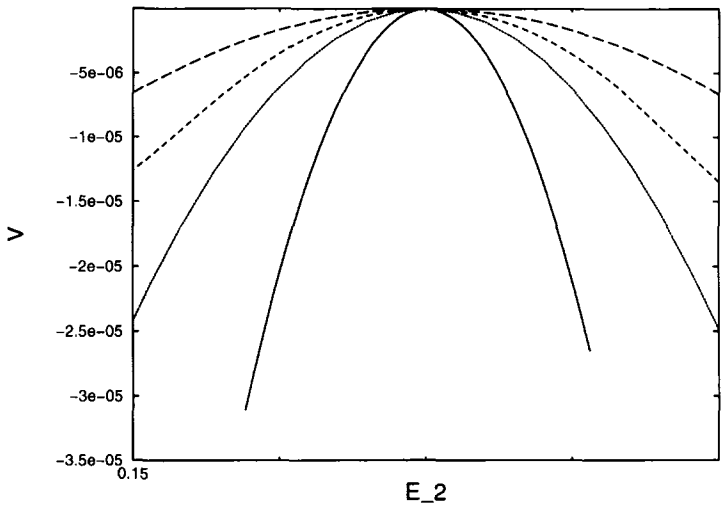

Fig. 11. Approach of effective potential of E_2 to zero for increasing σ. $\sigma=3$ (solid), $\sigma=4$ (dotted), $\sigma=5$ (short dash), $\sigma=6$ (long dash).

pointwise as $\sigma \to 0$. This is illustrated in Fig. 11 for E_2, but similar behavior is found as well for E_1 and T. This may be understood in the following way: for *all* values of σ the $N = 3$ Hermite-expansion *Ansatz* underestimates E_1 and T and overestimates E_2. The values closest to DNS are indeed obtained in the limit $\sigma \to \infty$, as the optimization principle predicts. It may be a little disturbing that realizability is still violated for V_{E_2} and V_T at every finite value of σ, although the predictions are off by as little as 0.17% from the DNS values! This indicates perhaps an oversensitivity of the effective potential realizability conditions here to departure from convergence. This is, however, the only example we have found so far in which the potentials exhibit such strong sensitivity. Furthermore, it is appropriate to point out that realizability is (marginally) recovered at the optimum point $\sigma = \infty$, since the potential is then $V \equiv 0$. This potential is indeed nonnegative and convex, although in a degenerate way. Hence, the realizability criterion would here also lead one to select correctly $\sigma = \infty$ as the best value.

We have studied as well some higher values of N, but the situation does not change qualitatively up to $N = 5$. The plateau values of the means are now

$$E_1^{(5,\infty)} = 2.0374 \tag{56}$$

$$E_2^{(5,\infty)} = 0.24948 \tag{57}$$

$$T^{(5,\infty)} = 0.49796 \tag{58}$$

The potentials are still all negative and concave, approaching the identically-zero potential pointwise as $\sigma \to \infty$. Hence, the above plateau values are again selected (correctly) as optimum values. The only difference from the $N = 3$ case is that the optimum predicted values are in better agreement with DNS for $N = 5$, just as one should expect. Although the Hermite-expansion method is not very successful up to $N = 5$, the realizability criterion and the optimization principle both correctly indicate how the best results may be obtained within that *Ansatz* for the nonequilibrium system.

It would be of interest to study even larger N, to test for ultimate convergence. However, using the direct-method eigenvalue routines in MATLAB, we were unable to consider $N > 5$ (corresponding to matrices of rank 343 or higher). Because the matrix in Eq. (46) is very sparse, iterative methods should allow one to go to higher values of N. We attempted to use the iterative Arnoldi method, which calculates selected eigenvalues and eigenvectors within Krylov subspaces (see ref. 37). This is particularly suited to finding eigenvalues of large, sparse, nonsymmetric matrices at the

extreme points of their spectra and also the associated eigenvectors. The computer time and memory requirements grow linearly with the rank of the matrix, here $R=(N+1)^3$, when the matrix has a sparse structure. The public-domain software ARPACK[38] contains Fortran programs to execute the Arnoldi algorithm. We used the ARPACK driver program *dndrv1.f*, a double-precision code for nonsymmetric matrices, to search for the principal eigenvalue $\lambda_{N,\sigma}(\mathbf{h})$ of the matrices in Appendix III.1, from which the effective potential could be constructed. In test runs for the equilibrium system, convergence was rapidly obtained using the ARPACK code for values of N up to 20. However, in the nonequilibrium system, we failed to get convergence for any value of N considered, even $N=1$. The reason seemed to be a failure to input a sufficiently good initial guess for the "right trial state," or stationary PDF. We tried both a simple Gaussian initial guess (all Hermite expansion coefficients $\beta_{\mathbf{n}}=0$ except $\beta_{\mathbf{0}}=1$) and also random choices of the $\beta_{\mathbf{n}}$. In all cases, the specified maximum number of iterations (20,000) was exceeded. This failure underscores the inadequacy of systematic Hermite expansions of PDF's in high Reynolds number turbulence applications. Even for this three mode system, expanding around a Gaussian *Ansatz* in orthogonal Hermite polynomials is a very poor way to represent the PDF far from absolute thermal equilibrium.

(iii) Near-Equilibrium Cascade

Our interest, of course, is not in the Hermite-expansions themselves, but rather in using them to investigate the utility of the variational method for a dissipative, non-equilibrium system. In principle, it should be possible to devise better initial guesses for the Arnoldi iteration, using the more successful PDF *Ansätze* from the following sections. However, it was easier simply to change the parameter values to be nearer to absolute equilibrium. *Therefore, in this section only we consider the choice of parameters*: $A_1=2$, $A_2=A_3=-1$, $\kappa_1=1.05$, $\kappa_2=\kappa_3=1.00$, $\nu_1=1.00$, $\nu_2=\nu_3=1.05$. This is still an irreversible cascade-state, but with statistics much closer to Gaussian. From DNS, the mean values are found to be:

$$E_1^{(DNS)}=0.509\pm 0.002 \tag{59}$$

$$E_2^{(DNS)}=0.483\pm 0.0001 \tag{60}$$

$$T^{(DNS)}=-0.0156\pm 0.0002 \tag{61}$$

The small magnitude of the triple moment is a quantitative measure of the nearness to Gaussianity. In this near-equilibrium case, the modal Reynolds numbers are all of order unity: $Re_1\approx 2.02$ and $Re_2=Re_3\approx 0.937$.

As for the equilibrium case, we obtained convergence of the Hermite expansions using the ARPACK code for N up to 20 and for a wide range of σ values in the near-equilibrium cascade. In fact, 8-decimal accuracy was obtained already at $N=12$ for σ near to 1, based upon comparison with the values for the next N. The results for the mean values so obtained were

$$E_1^{(Herm)} = 0.50955238 \tag{62}$$

$$E_2^{(Herm)} = 0.48354649 \tag{63}$$

$$T^{(Herm)} = -1.5447624 \times 10^{-2} \tag{64}$$

As may be seen, the agreement with the DNS for the means is well within numerical error. In Figs. 12–14 are plotted also the effective potentials of E_1, E_2 and T calculated from the Hermite expansion for $N=6$ (accurate to 3 decimals), along with the potentials obtained from DNS. Again, excellent agreement is obtained.

Even more interesting are the results of applying the optimization principle. For all N and σ studied, the Rayleigh–Ritz potentials satisfied the realizability constraints. Furthermore, in the range of σ considered, 0.7–1.1, the mean values exhibited stationary points as functions of σ, clear candidates for "optimum values." In Fig. 15 we plot the mean energy E_1 as a function of σ for N from 4 to 7, and, again, in Fig. 16 for N from 6 to 12. Similiar plots are obtained for E_2 and T. The rather strong dependence of

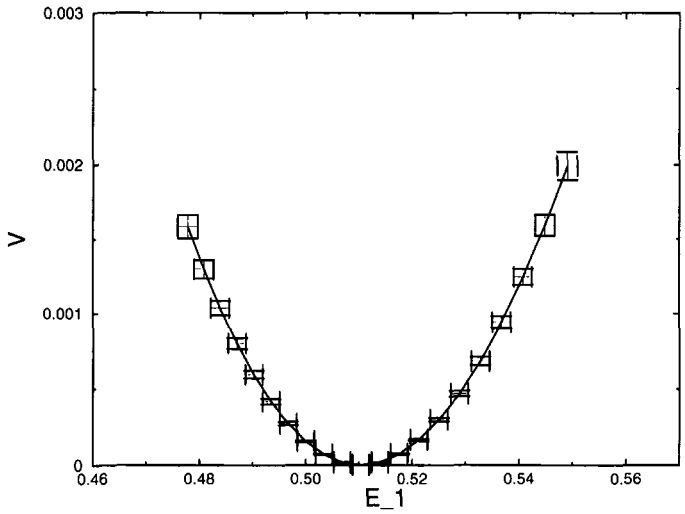

Fig. 12. Effective potential of E_1 in the near-equilibrium system with Hermite expansion, $N=6$, $\sigma=0.85$ and with DNS. DNS with error bars.

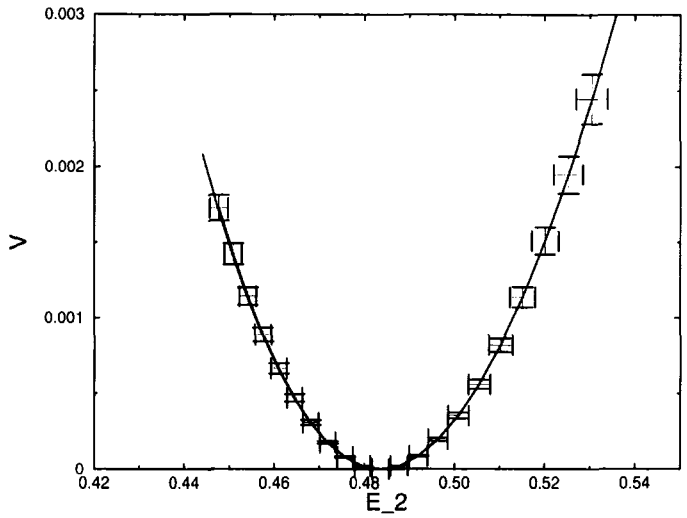

Fig. 13. Effective potential of E_2 in the near-equilibrium system with Hermite expansion, $N=6$, $\sigma=0.85$ and with DNS. DNS with error bars.

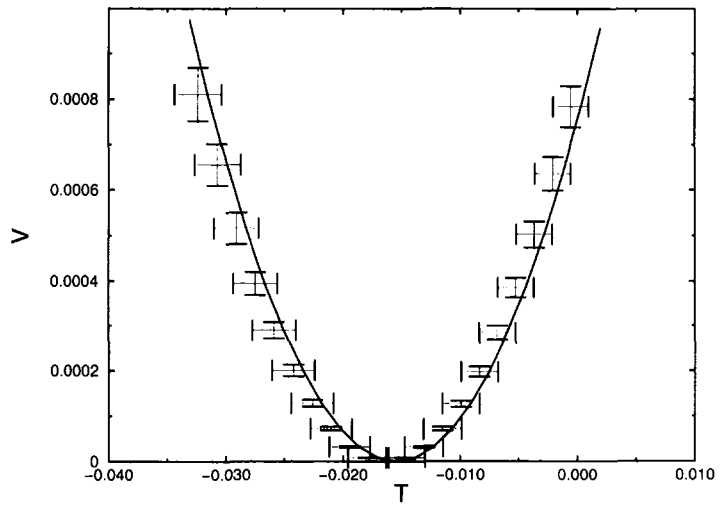

Fig. 14. Effective potential of T in the near-equilibrium system with Hermite expansion, $N=6$, $\sigma=0.85$ and with DNS. DNS with error bars.

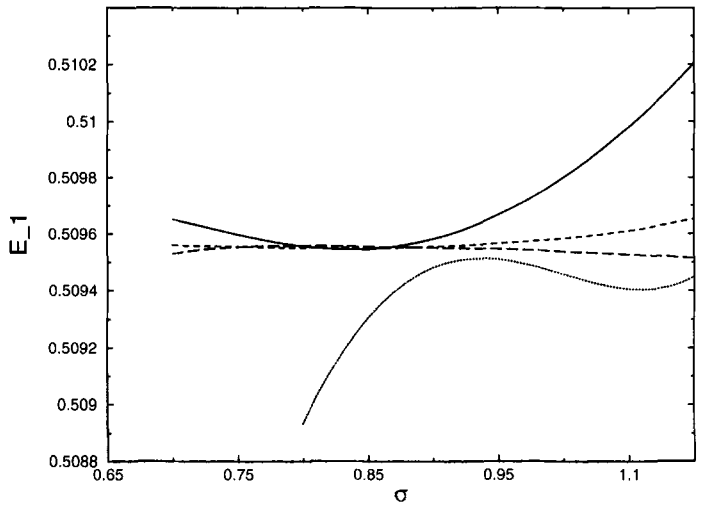

Fig. 15. Mean of E_1 vs. σ in the Hermite expansion for the near-equilibrium system, $N = 4$–7. $N = 4$ (solid), $N = 5$ (dotted), $N = 6$ (short dash), $N = 7$ (long dash).

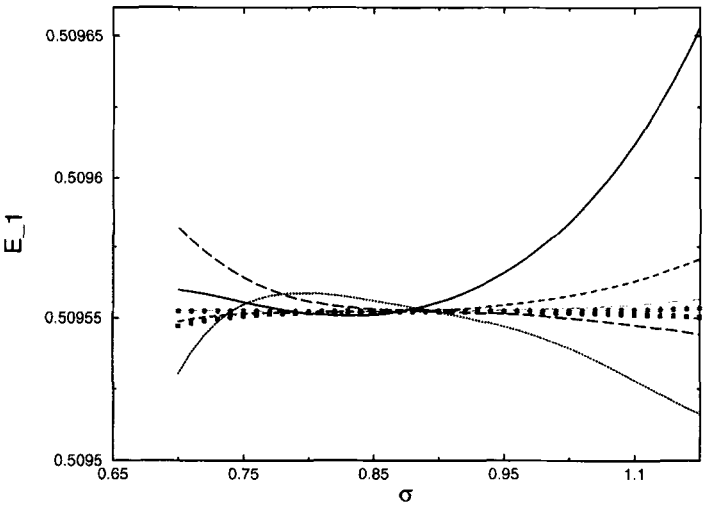

Fig. 16. Mean of E_1 vs. σ in the Hermite expansion for the near-equilibrium system, $N = 6$–12. $N = 6$ (solid), $N = 7$ (dotted), $N = 8$ (short dash), $N = 9$ (long dash), $N = 10$ (light dash), $N = 11$ (squares), $N = 12$ (circles).

the optimum values $\sigma^*(N)$ on the Hermite degree N is a little surprising, although the dependence is less for larger N. In any case, it is already clear from Figs. 15 and 16 that the candidate "optimum values" of energy-1 at each N, or $E_1^*(N)$, are closer to the final exact result than on the average; i.e. for typical fixed σ values independent of N.

This observation is borne out numerically. The optimum values $\sigma^*(N)$ were obtained at each N by the criterion that the local variation of the mean E_1 with respect to σ at that value be a minimum (if not zero) over the range considered. That is, the means were selected to have "minimal sensitivity" to the free parameter. These were compared with the predicted mean for one value of σ in the interval, fixed independent of N. We chose the equilibrium value of $\sigma = 1$ for this comparison, although other choices lead to similiar results. In the following Table 1 we give the results for the "optimum values" of energy at each N, or $E_1^*(N)$, along with the corresponding results for $\sigma = 1$, denoted simply $E_1(N)$. It has been checked that the "optimal values" of σ make the potential functions V_{E_1} nearly stationary to small variations of σ. Entirely similiar results are obtained also for $E_2 = E_3$ and T, which are therefore not shown.

It may easily be seen that the convergence is faster for the optimum values than it is for the fixed-sigma ($\sigma = 1$) values. This can be made more precise by considering the relative error

$$\Delta(N) \equiv \frac{|E(N) - E_{exact}|}{E_{exact}} \tag{65}$$

for each case, as displayed in Table 2. The relative error at $\sigma = 1$ for increasing N decreases roughly exponentially, i.e. $\Delta_1(N) \sim K^{-N}$, with $K = 2.7$–2.1. Interestingly, the convergence rate for the optimal values is less regular and not even monotonic. However, the relative errors of the optimal values are always smaller than those for fixed $\sigma = 1$, by a factor of

Table 1. Comparison of $\sigma = 1$ Values with Optimum Values

$E_1(4) = 0.50980117$	$E_1^*(4) = 0.50954617$
$E_1(5) = 0.50945790$	$E_1^*(5) = 0.50951379$
$E_1(6) = 0.50958394$	$E_1^*(6) = 0.50955085$
$E_1(7) = 0.50953943$	$E_1^*(7) = 0.50955870$
$E_1(8) = 0.50955776$	$E_1^*(8) = 0.50955201$
$E_1(9) = 0.50954997$	$E_1^*(9) = 0.50955242$
$E_1(10) = 0.50955345$	$E_1^*(10) = 0.50955236$
$E_1(11) = 0.50955188$	$E_1^*(11) = 0.50955237$
$E_1(12) = 0.50955262$	$E_1^*(12) = 0.50955238$

Table 2. Comparison of Relative Errors for $\sigma = 1$ and Optimum $\sigma^*(N)$

$\Delta_1(4) = 4.9 \times 10^{-4}$	$\Delta_1^*(4) = 1.2 \times 10^{-5}$
$\Delta_1(5) = 1.8 \times 10^{-4}$	$\Delta_1^*(5) = 7.6 \times 10^{-5}$
$\Delta_1(6) = 6.2 \times 10^{-5}$	$\Delta_1^*(6) = 3.0 \times 10^{-6}$
$\Delta_1(7) = 2.5 \times 10^{-5}$	$\Delta_1^*(7) = 1.2 \times 10^{-5}$
$\Delta_1(8) = 1.1 \times 10^{-5}$	$\Delta_1^*(8) = 7.3 \times 10^{-7}$
$\Delta_1(9) = 4.7 \times 10^{-6}$	$\Delta_1^*(9) = 7.8 \times 10^{-8}$
$\Delta_1(10) = 2.1 \times 10^{-6}$	$\Delta_1^*(10) = 3.9 \times 10^{-8}$
$\Delta_1(11) = 1.0 \times 10^{-6}$	$\Delta_1^*(11) = 2.0 \times 10^{-8}$

about 30 on the average. This is a clear success of the optimization principle. Note that a reduction of error by a factor of 30 at fixed $\sigma = 1$ would require going to a value of N higher by 3 or 4. Since the computational cost increases proportional to $\sim N^3$, it cheaper even for low values of N to search over a range of σ for an "optimum value" at fixed N. The same increase in accuracy is then obtained at considerably lower computational cost. This comparison would be even more dramatic for a system with many degrees of freedom D, since the cost of computation would then grow as $\sim N^D$.

We may summarize, finally, the results of this section. As expected, the representation of PDF's by Hermite polynomial expansions about Gaussian weights has very limited usefulness far from thermal equilibrium. However, the variational methods we have investigated make the best use of the poor choice of *Ansatz*. The realizability conditions on the effective potentials identify *a priori* the range of free parameters in which qualitatively correct predictions should lie. The optimization principle then pinpoints the best values of the parameters within that range (if any) at which the predictions are minimally sensitive to the change of free parameters. In the examples of this section, these criteria have led in each case to substantially improved quantitative predictions.

4. SECOND EXAMPLE: CHI-SQUARE PDF ANSATZ AND QUASINORMAL CLOSURE

In general, we do not expect it will be practical to look for convergence in far from equilibrium systems using systematic approximations, such as Hermite expansions. This is already true even for simple systems such as the 3-mode dynamics and even more likely in many degree-of-freedom systems such as Navier–Stokes dynamics. However, the Rayleigh–Ritz approximation of the potentials should still accurately reproduce the

exact ones, when calculated in conjunction with physically well-chosen PDF *Ansätze*. The best such models will not, in our opinion, be based upon rote analytical approximations of PDF's, but shall require a fair amount of insight into the dynamics and statistics of the system considered. It is crucial to test whether the effective potentials can be successfully calculated—for selected random variables—using such physically-motivated, but relatively crude, PDF *Ansätze*. If our ideas on using the effective potentials for practical turbulence modeling are correct, then the same closures able to calculate successfully the mean values must also be able to reproduce fairly well the fluctuations around the mean. Otherwise, there would be little practical interest to monitor the performance of the closures in describing the fluctuations.

We have therefore attempted to calculate effective potentials of the nonequilibrium 3-mode system by adopting appropriate statistical "surrogate" variables for the three modal variables. The closure we first considered is borrowed from an unpublished work of Bayly.[39] It can be regarded as a simple type of mapping closure, with the realizations of the 3-modes represented by a quadratic map $\mathbf{X} = \mathbf{Q}[\mathbf{N}, \mathbf{N}']$ of 6 independent, identically distributed normal random variables $\mathbf{N} = (N_1, N_2, N_3)$, $\mathbf{N}' = (N_1', N_2', N_3')$, each of zero mean and standard deviation 1. More precisely, the so-called *chi-square Ansatz* is specified as

$$X_i = \beta_i N_i + \beta_4 N_j' N_k' \tag{66}$$

with i, j, k a cyclic permutation of 1, 2, 3. This *Ansatz* contains 4 closure parameters $\boldsymbol{\beta} = (\beta_1, \beta_2, \beta_3, \beta_4)$. The terminology "chi-square" arises from mathematical statistics, where the product of two Gaussian random variables is called a χ^2 random variable. Such variables have strongly non-Gaussian PDF's, with exponential tails. Hence, the quadratic terms proportional to β_4 are responsible in this *Ansatz* for the non-Gaussian effects, such as energy transfer. To determine the 4 closure parameters a corresponding set of 4 moment-functions $\boldsymbol{\psi} = (\psi_1, \psi_2, \psi_3, \psi_4)$ are required. These are taken to be

$$\psi_i(\mathbf{x}) = x_i^2 \tag{67}$$

for $i = 1, 2, 3$ and

$$\psi_4(\mathbf{x}) = x_1 x_2 x_3 \tag{68}$$

The associated moments $\boldsymbol{\mu} = \langle \boldsymbol{\psi} \rangle$ are easily calculated within the previous *Ansatz* Eq. (66):

$$\mu_i = \beta_i^2 + \beta_4^2 \tag{69}$$

for $i=1, 2, 3$ and

$$\mu_4 = \beta_4^3 \tag{70}$$

These moments are directly related to the modal energies $E_i = \frac{1}{2}\mu_i$, $i=1, 2, 3$ and the triple correlation $T=\mu_4$. There are no free parameters in the χ^2 *Ansatz*.

The resulting closure equations are easily derived as

$$\dot{\mu}_i = 2A_i\mu_4 - 2\nu_i\mu_i + 2\kappa_i \tag{71}$$

for $i=1, 2, 3$ and

$$\dot{\mu}_4 = A_1\mu_2\mu_3 + A_2\mu_1\mu_3 + A_3\mu_1\mu_2 - (\nu_1+\nu_2+\nu_3)\mu_4 \tag{72}$$

These are just the *quasinormal closure equations* of Proudman and Reid[40] written for the 3-mode model, which are obtained by the neglect of 4th-order cumulants in the equation for the 3rd-order moment. The χ^2 PDF *Ansatz* actually gives non-vanishing cumulant parts to the 4th-order correlations appearing in the equation for μ_4, namely $\langle X_i^2 X_j^2\rangle = \mu_i\mu_j + 2\mu_4^{4/3}$ for $i\neq j$. However, the 4th-order cumulant terms drop out of the equation for μ_4 as a result of the conservation condition $A_1+A_2+A_3=0$. The quasinormal (QN) equations have some special interest since they were historically the first example to yield a violation of realizability of 2nd-order moments. The possibility of negative energy spectra was observed by Kraichnan[4, 5] and negative values were in fact obtained in some wavenumber ranges by Ogura[41, 42] in a numerical solution of the QN equations for 2D and 3D Navier–Stokes. This example led Kraichnan to raise the general issue of realizability in turbulence modeling.[4, 5]

In his 1963 paper on the 3-mode model[20] Kraichnan observed, on the other hand, that the QN equations for that system seem to be realizable and lead there to positive modal energies. There are actually two fixed points of the QN equations for the 3-mode model, one with all positive energies but another with some negative energies. The fixed points energies are obtained from

$$\mu_i = \frac{A_i\mu_4 + \kappa_i}{\nu_i} \tag{73}$$

for $i=1, 2, 3$ with μ_4 determined as one of the two roots of the quadratic equation

$$a\mu_4^2 + b\mu_4 + c = 0 \tag{74}$$

for

$$a = (\nu_1 + \nu_2 + \nu_3)\, A_1 A_2 A_3 \tag{75}$$

$$b = \nu_1 A_1 (A_2 \kappa_3 + A_3 \kappa_2) + \nu_2 A_2 (A_1 \kappa_3 + A_3 \kappa_1) + \nu_3 A_3 (A_1 \kappa_2 + A_2 \kappa_1) - \nu_1 \nu_2 \nu_3 (\nu_1 + \nu_2 + \nu_3) \tag{76}$$

$$c = \nu_1 A_1 \kappa_2 \kappa_3 + \nu_2 A_2 \kappa_1 \kappa_3 + \nu_3 A_3 \kappa_1 \kappa_2 \tag{77}$$

The fixed point with some energies negative is found to be unstable, while the fixed point with all positive energies is stable. The stable fixed point with positive energies thus satisfies all of the standard realizability conditions and it is of particular interest to see how it fares under our new realizability criterion. For our standard nonequilibrium choice of parameters we find at the stable QN fixed point the values

$$\mu_1^{(QN)} = 1.4987506 \tag{78}$$

$$\mu_2^{(QN)} = \mu_3^{(QN)} = 0.5002506247 \tag{79}$$

$$\mu_4^{(QN)} = -0.4992506247 \tag{80}$$

These may be compared with the DNS values

$$\mu_1^{(DNS)} = 4.46 \pm 0.05 \tag{81}$$

$$\mu_2^{(DNS)} = \mu_3^{(DNS)} = 0.49877 \pm 0.00003 \tag{82}$$

$$\mu_4^{(DNS)} = -0.49777 \pm 0.00005 \tag{83}$$

We see that the 2nd, 3rd, and 4th moments are well-predicted by the QN closure, but the 1st moment is badly underpredicted. Examination of the Eq. (73) for $i = 1$ shows that the reason for this poor prediction is the near cancellation between the two terms in the numerator, which implies that a very accurate value for μ_4 is required to obtain an adequate value for μ_1.

An interesting point is that the fixed point considered, while stable and giving positive energies, is actually not realizable within the χ^2-*Ansatz*. A simple calculation shows that the above fixed point values require $\beta_2^2 = \beta_3^2 = -0.129080307$, which leads to a *pure imaginary* value of $\beta_2 = \beta_3$! On the other hand, the fixed-point value of β_1 is obtained from $\beta_1^2 = 0.8694197$ and is thus real. Although the χ^2 PDF is not realizable for the fixed point values, the closure actually does a quite adequate job of predicting $\mu_2 = \mu_3$ and μ_4. From the fact that the fixed point β_i value is imaginary for $i = 2, 3$ and real for $i = 1$, one might be misled into believing that the predictions are good for μ_1 and poor for $\mu_2 = \mu_3$. However, the opposite is the case.

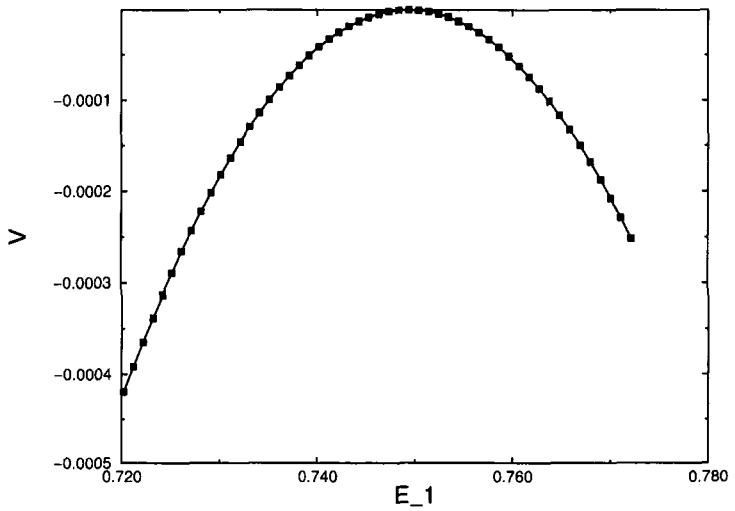

Fig. 17. Effective potential of E_1 in the nonequilibrium system with the chi-square ansatz curve is negative and concave, violating realizability.

We now consider the approximate effective potentials of the variables $E_i(\mathbf{x}) = \frac{1}{2}x_i^2$ and $T(\mathbf{x}) = x_1x_2x_3$ within the χ^2-closure. The dynamical vector fields of the closure used in the Rayleigh–Ritz calculation are recorded in Appendix III.2. The results are graphed in Figs. 17–19. We see that the effective potentials V_T and $V_{E_2} = V_{E_3}$ satisfy all the realizability conditions. However, the effective potential V_{E_1} is negative and concave, violating realizability. Thus, based upon our realizability criterion, we would be led *a priori* to reject the QN prediction for E_1 but, at least tentatively, to accept the predictions for $E_2 = E_3$ and T. Hence, the realizability criterion based upon the approximate effective potentials is successful here. As we have already observed, the classical realizability conditions on energies are all satisfied in this case and do not detect the poor prediction of E_1. Furthermore, while the realizability of the full PDF for the χ^2 *Ansatz* certainly fails, the source of failure actually tends to mislead regarding which predictions are good and which poor. By contrast, the effective potential here has accurately pinpointed the good predictions for $E_2 = E_3$ and T and the bad one for E_1. It is interesting to decompose the χ^2 approximate effective potential $V_{E_1}(e)$ into 4 terms corresponding to each of the 4 moment-functions of the closure:

$$V_{E_1}(e) = \sum_{i=1}^{4} V_{E_1}^{(i)}(e) \tag{84}$$

where

$$V_{E_1}^{(i)}(e) = -\alpha_{*i}(h_{*1}(e))\, V_i(\mu_*(h_{*1}(e))) \tag{85}$$

for $i = 1, 2, 3, 4$, and the various expressions therein are given in Appendix III(ii). We have checked that the separate terms are all positive and convex except the $i = 4$ term, which is the dominant contribution and leads to the overall realizability-violating potential. It is the role played by transfer in the χ^2 *Ansatz* which is leading to the nonrealizable potential for E_1.

For the two variables whose effective potentials satisfy realizability in the χ^2 *Ansatz* it is interesting to compare with the potentials obtained from DNS. The results from DNS are graphed along with the χ^2 predictions from Rayleigh–Ritz in Figs. 18 and 19 for V_{E_2} and V_T. It is seen that the results are qualitatively in agreement. In fact, quantitatively the χ^2 results agree with those from DNS to about 30% over a range of variation of about 20% from the mean value. This is a very satisfactory agreement, given the crudity of the closure. It is significant that such a reasonable agreement is obtained in the Rayleigh–Ritz calculation, despite the breakdown of realizability of the PDF *Ansatz* itself. This indicates that the effective potentials are more robust measures of correctness of predictions than the PDF. These results are an important test of our ideas on practical

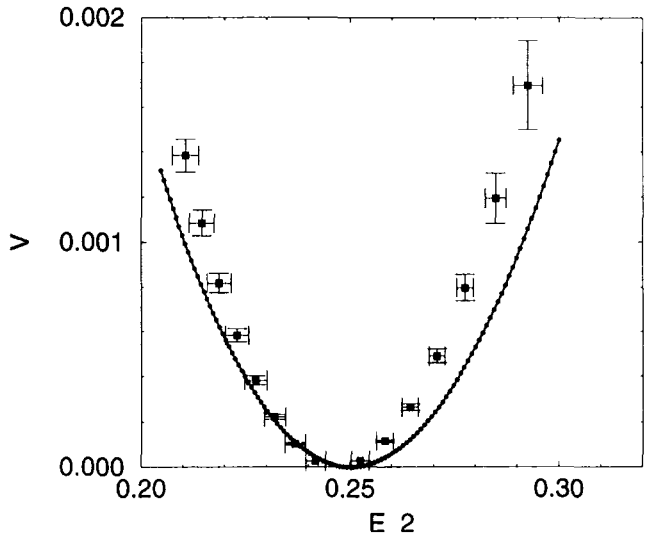

Fig. 18. Effective potential of E_2 in the nonequilibrium system with the chi-square ansatz and with DNS. DNS with error bars.

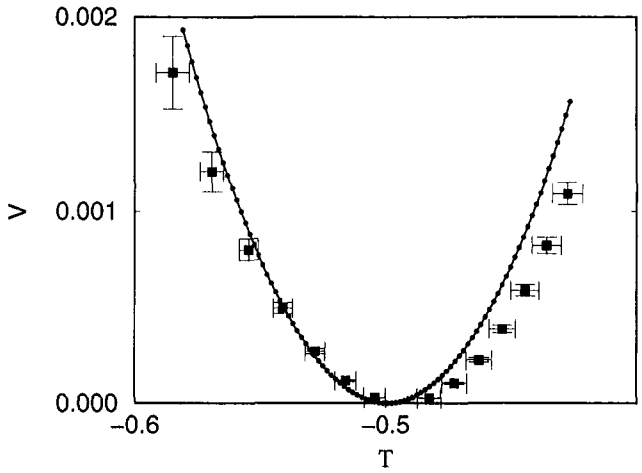

Fig. 19. Effective potential of T in the nonequilibrium system with the chi-square ansatz and with DNS. DNS with error bars.

modeling. The utility of the realizability criterion on effective potentials depends upon the thesis that an *Ansatz* adequate to calculate a mean-value should also yield a reasonable result for the fluctuations, as codified in the effective potentials. The inverse statement then must hold as well: a qualitatively poor prediction for the fluctuations should imply also a poor prediction for the mean.

We briefly discuss some other results for the χ^2 PDF closure:

As pointed out earlier, it is not really meaningful to employ the Rayleigh–Ritz approximation of potentials at an unstable fixed point. Nevertheless, out of academic interest we have done so at the unstable fixed point in the χ^2-closure and we report the results briefly here. The moments at this second unstable fixed point are $\mu_1^{(\text{unst})} = 1002.001999$, $\mu_2^{(\text{unst})} = \mu_3^{(\text{unst})} = -000000995$, $\mu_4^{(\text{unst})} = 0.0010009995$. The predicted energies of modes-2 and 3 are negative at this fixed point, violating 2nd-moment realizability. It is amusing to note, however, that the Rayleigh–Ritz potentials of $V_{E_2} = V_{E_3}$ are positive and convex, satisfying realizability! On the other hand, the potential V_T is realizability-violating: see Fig. 20. Thus, even if one (incorrectly) ignored the instability of the second fixed point and its failure of 2nd-moment realizability, the effective potential for V_T calculated by Rayleigh–Ritz would reveal a problem.

Although we have focused in this section on the nonequilibrium cascade states, the χ^2-closure can also be applied to the equilibrium system. In Fig. 21 we plot the effective potential V_{E_1} for the equilibrium case calculated by Rayleigh–Ritz in the χ^2 *Ansatz*, versus the result for the

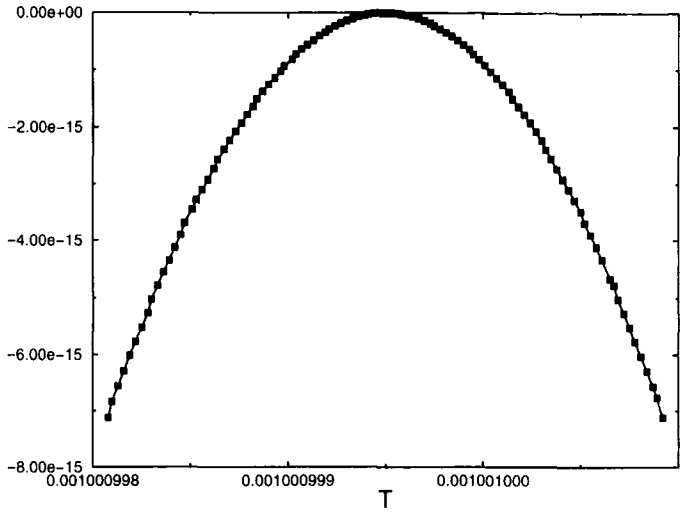

Fig. 20. Effective potential of T with the unstable fixed point of the chi-square closure. Curve is negative and concave, violating realizability.

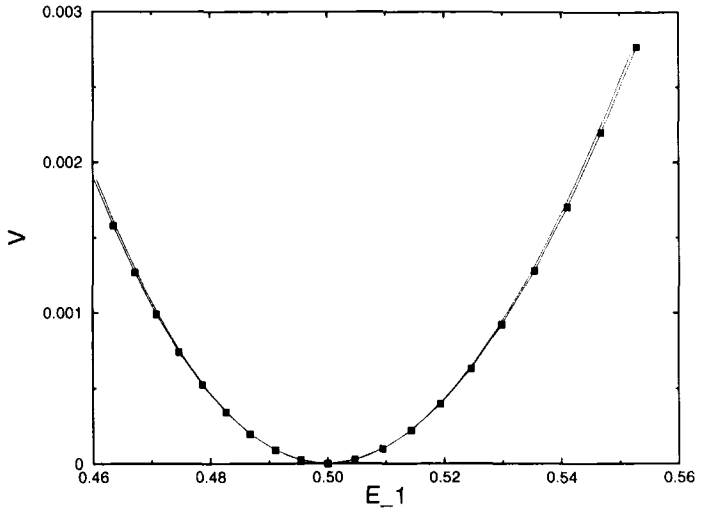

Fig. 21. Effective potential of energy in the equilibrium system with the chi-square ansatz and with Hermite, $\sigma = 1$, $N = 3$. Chi-square (squares), Hermite (solid line).

Hermite-expansion, $N=3$, $\sigma=1$, which is essentially exact in the range considered. As one can see, the two are indistinguishable over an interval in which the energy varies up to 10% from the mean value. This is a remarkable success of the χ^2-closure, considering that there are 64 parameters in the $N=3$ Hermite-expansion PDF and only 5 (counting μ_0) in the χ^2 *Ansatz*! Hence, this closure works very well for the equilibrium system and, in the nonequilibrium case, gives good predictions of T and $E_2=E_3$. The chief failing of the χ^2-*Ansatz* is really only in its miscalculation of the mode-1 energy in the nonequilibrium cascade system.

5. THIRD EXAMPLE: TWISTED-GAUSSIAN PDF ANSATZ

We have not yet developed in this paper any PDF *Ansatz* which is adequate to calculate all of the relevant statistics of the nonequilibrium cascade states for the 3-mode system. In general, one hopes that it will be possible to make *Ansätze* adequate to describe some low-order statistics of interest, by combining data from experiments and simulation, physical insights, and basic mathematical constraints. Thus, it is of interest here to test that idea, by trying to develop a model PDF which can better calculate the mean energy E_1 (the main failure of the χ^2 *Ansatz*), along with the other mean statistics. If so, then it is important to examine whether realizability will hold for the corresponding potential V_{E_1}. If realizability holds, then it is furthermore interesting to see how quantitatively accurate is that approximate potential. To develop an improved model PDF for this purpose, one might try to add parameters systematically to the χ^2 *Ansatz*, e.g. by adding higher-order terms than quadratic in the mapping function $\mathbf{Q}$. However, we have instead considered a fundamentally different PDF model.

Recall that in the χ^2 *Ansatz* the fixed point was not realizable, with parameters β_i becoming pure imaginary for $i=2, 3$ and only β_1 remaining real. It is apparent from that result that only the 1-mode has a large Gaussian component and that the 2 and 3-modes are essentially non-Gaussian. Further insight into the character of their statistics is provided by DNS study of the system. In work of Bayly and Sochos,[43] scatterplots of the stationary PDF $P_s(\mathbf{x})$ of the 3-mode system were obtained from DNS. We have reproduced this work, with results illustrated in Fig. 22. The plots show that, with high probability, either $x_2 \approx x_3$ or $x_2 \approx -x_3$ in every realization. We therefore have adopted a model which incorporates these observations and, as well, has the required statistical symmetries (discussed in Appendix 1). This *twisted-Gaussian* (*TG*) model represents the realizations of the 3-mode system by

$$X_1 = \beta_1 N_1 \tag{86}$$

$$X_2 = \theta^+(N_1)[\beta_2 B N_2 + \beta_3(1-B) N_3] + \theta^-(N_1)[\beta_2 B N_2 - \beta_3(1-B) N_3] \tag{87}$$

$$X_3 = \theta^+(N_1)[\beta_2 B N_2 + \beta_3(1-B) N_3] + \theta^-(N_1)[\beta_2 B N_2 - \beta_3(1-B) N_3] \tag{88}$$

where N_1, N_2, N_3 are as before independent standard normal random variables, the Heaviside theta functions $\theta^{\pm}$ are defined by

$$\theta^+(x) = \begin{cases} 1 & x > 0 \\ 0 & x < 0 \end{cases} \quad \text{and} \quad \theta^-(x) = \begin{cases} 0 & x > 0 \\ 1 & x < 0 \end{cases} \tag{89}$$

and B is a Bernoulli random variable; i.e. $B = 1$ with probability p and $B = 0$ with probability $q = 1 - p$. Thus, the variable X_1 is represented entirely by a Gaussian. Furthermore, in this model, for $X_1 > 0$, $X_2 = X_3 = \beta_2 N_2$ with probability p and $X_2 = -X_3 = \beta_3 N_3$ with probability q, while for $X_1 < 0$, $X_2 = -X_3 = \beta_2 N_2$ with probability p and $X_2 = X_3 = -\beta_3 N_3$ with probability q. This *Ansatz* is faithful to the main features observed in the scatterplots and has all the required statistical symmetries. Unlike the χ^2 *Ansatz* (which includes the Gaussian PDF as a special case when $\beta_4 = 0$), this closure would not work well for the equilibrium system and is tailored fundamentally to the nonequilibrium cascade states.

The TG-*Ansatz* contains three closure parameters $\boldsymbol{\beta} = (\beta_1, \beta_2, \beta_3)$ as well as one free parameter p. To fix the closure parameters three test functions $\boldsymbol{\psi} = (\psi_1, \psi_2, \psi_3)$ are required. We have chosen

$$\psi_1(\mathbf{x}) = x_1^2 \tag{90}$$

$$\psi_2(\mathbf{x}) = x_2^2 \tag{91}$$

$$\psi_3(\mathbf{x}) = x_1 x_2 x_3 \tag{92}$$

from which one easily calculates the corresponding moments $\boldsymbol{\mu} = \langle \boldsymbol{\psi} \rangle$ as

$$\mu_1 = \beta_1^2 \tag{93}$$

$$\mu_2 = p\beta_2^2 + q\beta_3^2 \tag{94}$$

$$\mu_3 = \sqrt{\frac{2}{\pi}} \cdot \beta_1 (p\beta_2^2 - q\beta_3^2) \tag{95}$$

Note that $\langle X_2^2 \rangle = \langle X_3^2 \rangle$ in this *Ansatz*, just as for the exact stationary distribution when $\nu_2 = \nu_3$ and $\kappa_2 = \kappa_3$. Thus, it is not necessary to add x_3^2 as

a test function because of the exact statistical permutation symmetry of the 2 and 3-modes. Note also that a negative triple moment is obtained in the *Ansatz* when the "correlated bar" of the "cross" in the $X_2 - X_3$-plane is the longest and heaviest for $X_1 < 0$ and the "anticorrelated bar" is the longest and heaviest for $X_1 > 0$. This is the "twist," which reproduces rather well the features seen in the scatterplot of Fig. 22.

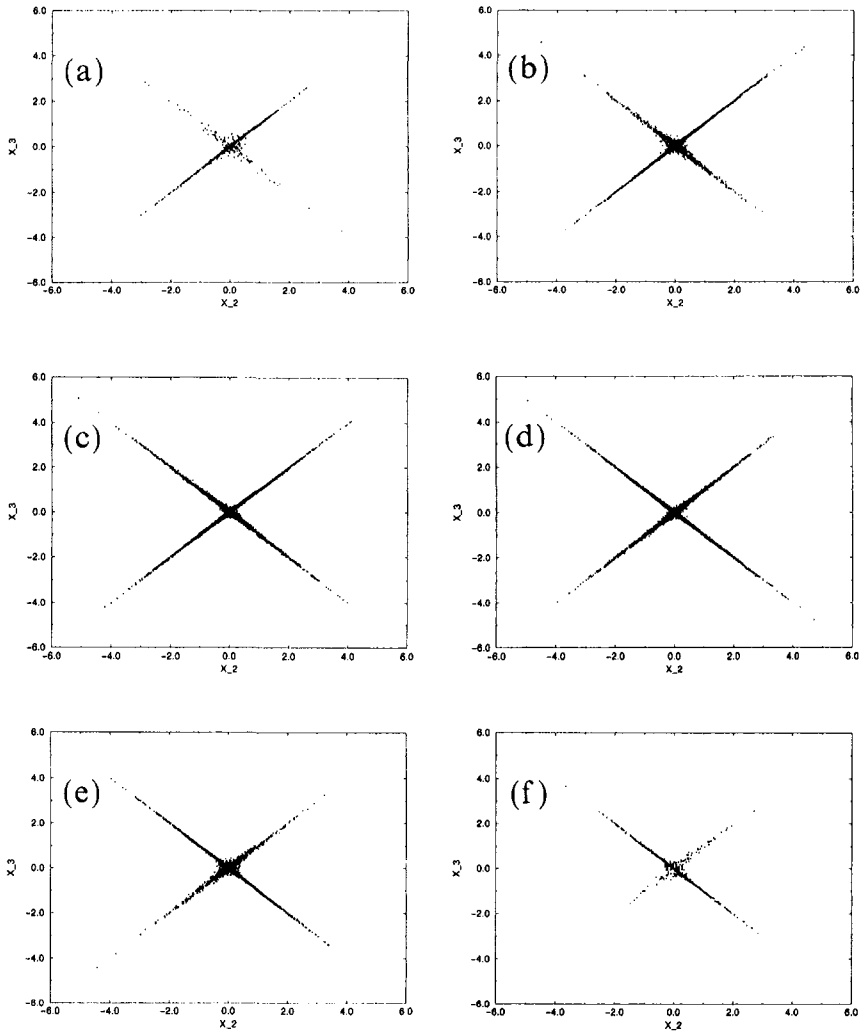

Fig. 22. Scatterplot of PDF in the nonequilibrium system. Shown are cuts in the (x_2, x_3)-plane at constant $x_1 = -5$ (a), $x_1 = -3$ (b), $x_1 = -1$ (c), $x_1 = 1$ (d), $x_1 = 3$ (e), $x_1 = 5$ (f).

The resulting closure equations for the moments $\boldsymbol{\mu}$ are easily obtained, as

$$\dot{\mu}_1 = 2A_1\mu_3 - 2\nu_1\mu_1 + 2\kappa_1 \tag{96}$$

$$\dot{\mu}_2 = 2A_2\mu_3 - 2\nu_2\mu_2 + 2\kappa_2 \tag{97}$$

$$\dot{\mu}_3 = \frac{3A_1}{4pq}\left[\mu_2^2 + \frac{\pi\mu_3^2}{2\,|\mu_1|} + (p-q)\sqrt{\frac{2\pi}{|\mu_1|}}\,\mu_2\mu_3\right] + (A_2+A_3)\,\mu_1\mu_2 - (\nu_1+\nu_2+\nu_3)\,\mu_3 \tag{98}$$

The absolute value signs $|\cdot|$ appearing on some μ_1 factors would be unnecessary if realizability of fixed points were guaranteed, so that the 2nd-moment μ_1 must be positive. The absolute values have been added here (somewhat arbitrarily) to all factors originating from a $\sqrt{\mu_1}$ to prevent imaginary values from appearing in the equations. (Without the absolute value signs an unstable fixed point with $\mathrm{Re}(\mu_1) < 0$ in fact appears.) We see that the only difference from the QN equations is in the modeling of the moment

$$\langle X_2^2 X_3^2\rangle = \frac{3}{4pq}\left[\mu_2^2 + \frac{\pi\mu_3^2}{2\,|\mu_1|} + (p-q)\sqrt{\frac{2\pi}{|\mu_1|}}\,\mu_2\mu_3\right] \tag{99}$$

which has, in addition to the term $\propto \langle X_2^2\rangle\langle X_3^2\rangle = \mu_2^2$, also a nontrivial cumulant part. The resulting closure equations thus contain a nonvanishing contribution from 4th-order cumulants.

In the steady-state, the first two equations may be used to eliminate μ_2 and μ_3 in the final equation in terms of μ_1 alone. There are two fixed points determined from this equation. For $p = 0.5$, the values are

$$\mu_1^{(I)} = 3.223735433, \quad \mu_2^{(I)} = 0.499388132, \quad \mu_3^{(I)} = -0.498388132 \tag{100}$$

at fixed point *I*, and

$$\mu_1^{(II)} = 1002.001999, \quad \mu_2^{(II)} = -0.000000999, \quad \mu_3^{(II)} = 0.001000999 \tag{101}$$

at fixed point *II*. Numerical spectral analysis of the Jacobian matrices at these fixed points shows that *I* is stable and *II* is unstable. Fixed point *I* is also the only one to satisfy standard 2nd-moment realizability, as μ_2 is negative for fixed point *II*. (Note, however, that the violation of 2nd-moment realizability is, in some sense, slight at fixed point *II*, as the value of μ_2 is quite close to 0.) In general for arbitrary values of p we find that the fixed points *I* and *II* exist with similar properties.

Because the fixed point I is stable and satisfies 2nd-moment realizability, it is the obvious candidate for the physical fixed point. Furthermore, it may easily be checked from Eqs. (93)–(95) that the parameters β_i, $i=1$, 2, 3 are real-valued at fixed point I for all p, and therefore PDF realizability is satisfied as well. Fixed point I of the TG-closure is the only one which we shall consider here. In Figs. 23–25 we plot the predictions for E_1, E_2, and T as a function of the free parameter p. We see that, although E_2 and T are only weakly dependent on p, the mean energy E_1 in mode-1 is much more strongly dependent on p. As p approaches either of its limiting values 0 or 1, all three rise or fall rapidly.

The minimum value of $E_1 \approx 1.25$ occurs at $p \approx 0.896$. This minimum is too shallow to be seen clearly on the original scale, but is shown on the inset graph of Fig. 23. Hence, the point $p_* \approx 0.896$ is a candidate for an "optimum" value of the free parameter p. However, we may note in advance that the mean energy E_1 at this point is considerably underpredicted, 45% smaller than the DNS value $E_1 \approx 2.28$. On the other hand, the predicted value of E_1 in the TG-closure for $p = p_*$ is still better than the QN prediction of $E_1 = 0.75$. In Fig. 26 we plot the potential of V_{E_1} in the TG-closure for $p = p_*$ and for nearby values of p. Clearly, it satisfies realizability and so also do the TG predictions for V_{E_2} and V_T (not shown). In fact, the same qualitative features are observed for V_{E_1}, V_{E_2} and V_T at *all* p-values in the TG-closure (see below). The Fig. 26 demonstrates

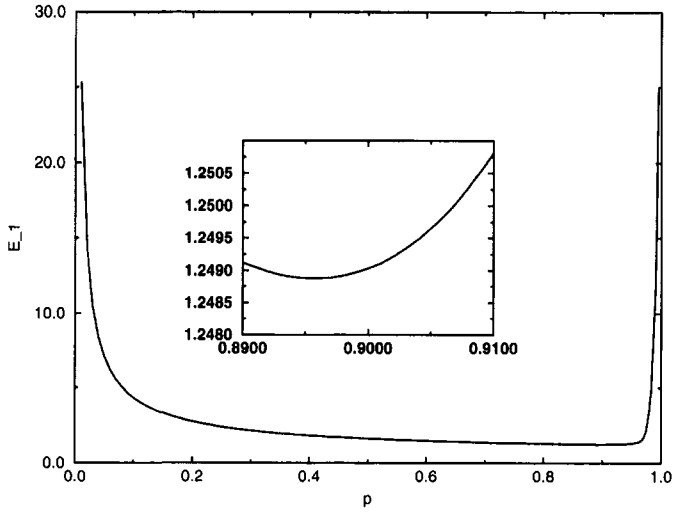

Fig. 23. Mean of E_1 vs. p in the twisted-Gaussian ansatz for the nonequilibrium system. The inset zooms into the neighborhood of the minimum at ≈ 0.896.

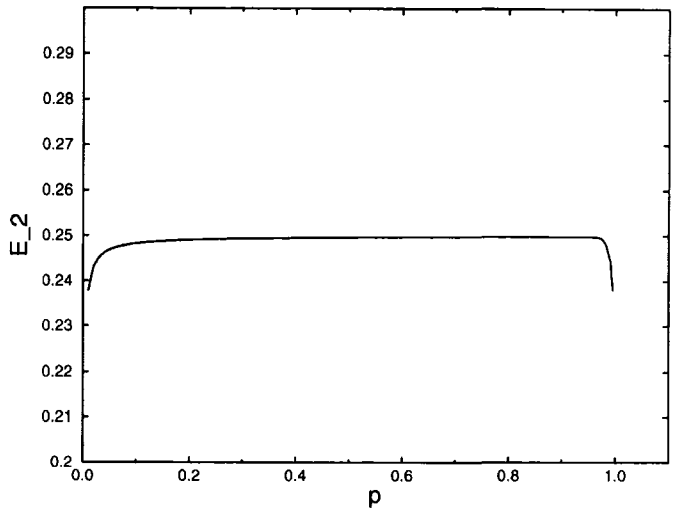

Fig. 24. Mean of E_2 vs. p in the twisted-Gaussian ansatz for the nonequilibrium system.

as well that V_{E_1} is nearly stationary to variations of p at the point $p = p_*$, at least in the interval of E_1 shown near the minimum. Hence, it should be taken as the "optimum value" of p according to the optimization principle. However, the prediction for E_1 at the parameter value $p = p_*$ is the *worst underprediction* over the whole range of p values! This illustrates vividly the

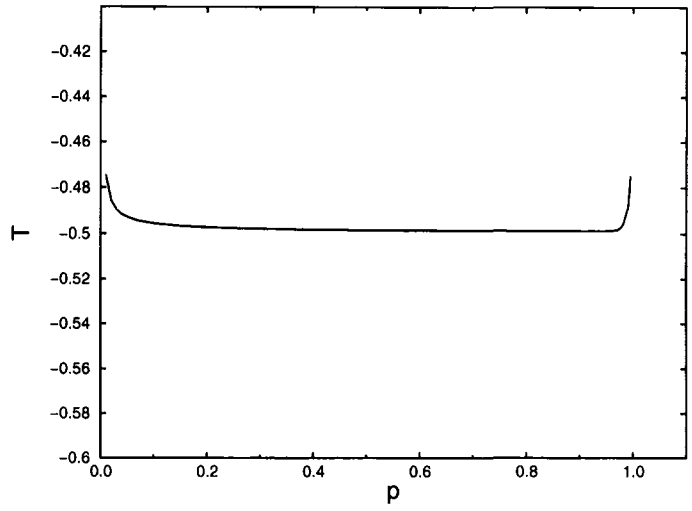

Fig. 25 . Mean of T vs. p in the twisted-Gaussian ansatz for the nonequilibrium system.

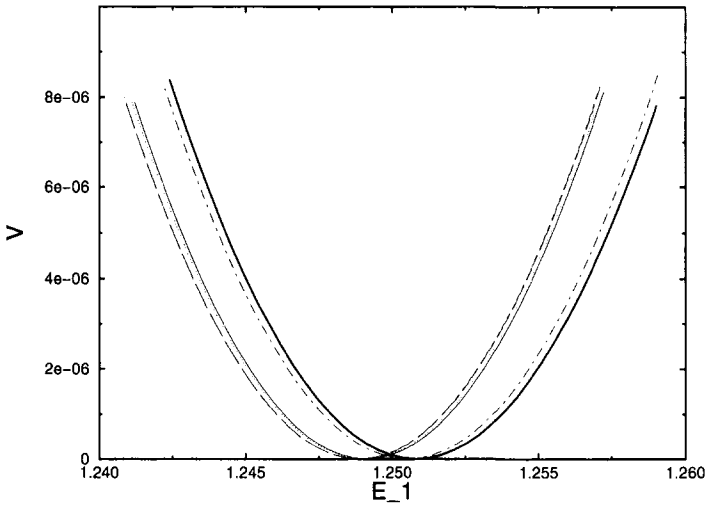

Fig. 26. Comparison of effective potentials under variation of p. *first group* $p = 0.896$ (short dash), $p = 0.897$ (long dash); *second group* $p = 0.91$ (light dash), $p = 0.909$ (heavy solid); *third group* $p = 0.890$ (light solid), $p = 0.891$ (dotted) $p = 0.896$ is clearly a stationary point.

important dictum that realizability cannot guarantee closeness to the true answer, as here the departure is up to 45% from DNS yet all realizability conditions are satisfied. However, the satisfaction of realizability is consistent with the qualitative correctness of the TG-closure, which is in line with its observed improvement over the χ^2-closure. A more serious limitation may be revealed in the optimization principle in this example. In defense of the principle it may be pointed out that much worse predictions are obtained in the TG-closure for $p \neq p_*$, e.g. near the endpoints $p = 0$ or $p = 1$. On the other hand, the predictions at $p = p_*$ are far from the best possible.

In fact, it is possible to make an *a posteriori* adjustment of the parameter p so that the mean values E_1, E_2 and T are exactly postdicted. There are found to be two distinct values, $p_- \approx 0.280$ or $p_+ \approx 0.975$, which reproduce the DNS values of all three means precisely. As we show in Figs. 27–29 the results at those two values for the potentials V_T are nearly indistinguishable, the corresponding V_{E_2} are also fairly close, but the calculated V_{E_1} are quite distinct. The smaller value $p = p_-$ reproduces better the features of the PDF seen in the scatterplots, so that we adopt it here. In Figs. 30–32 we compare the three potentials V_{E_1}, V_{E_2} and V_T obtained from TG for $p = p_-$ with those obtained from DNS. As may be seen, agreement is remarkably good over a range of values differing as much as 20% from the mean.

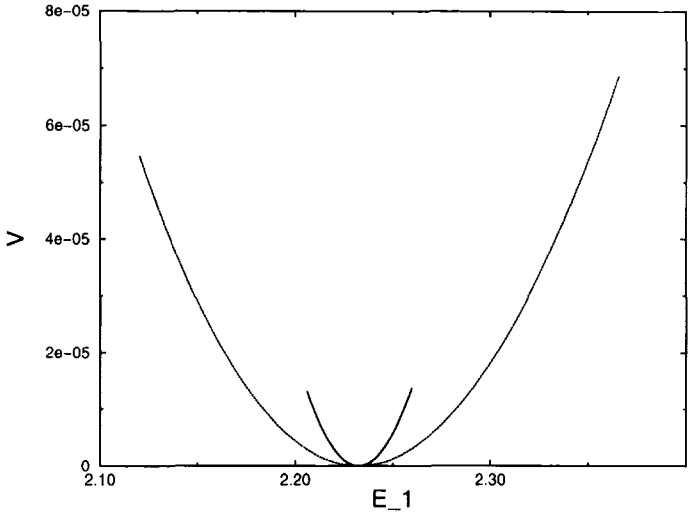

Fig. 27. Effective Potential of E_1 in the nonequilibrium system with the twisted-Gaussian ansatz, $p = p_+$ and $p = p_-$. $p = p_+$ (dotted), $p = p_-$ (solid).

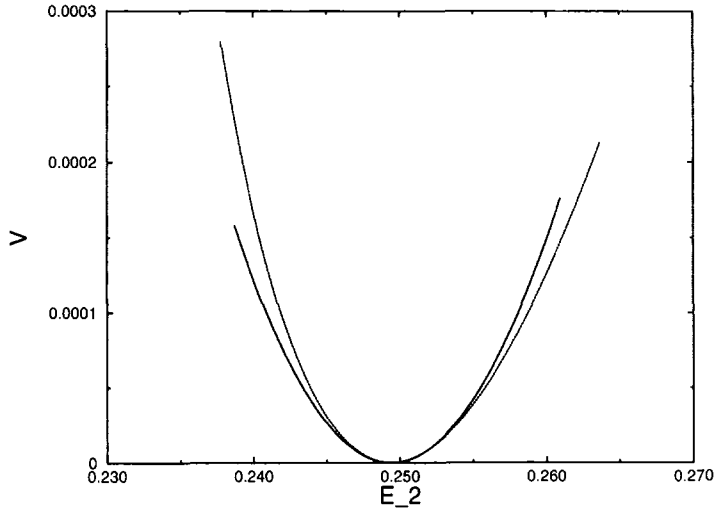

Fig. 28. Effective potential of E_2 in the nonequilibrium system with the twisted-Gaussian ansatz, $p = p_+$ and $p = p_-$. $p = p_+$ (dotted), $p = p_-$ (solid).

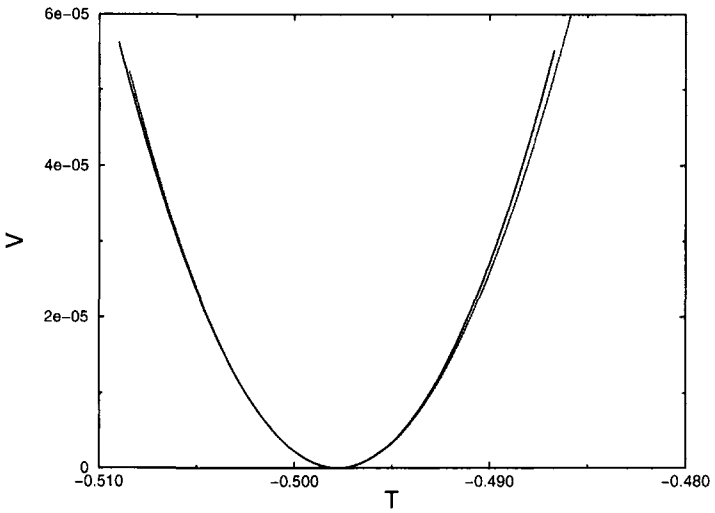

Fig. 29. Effective potential of T in the nonequilibrium system with the twisted-Gaussian ansatz, $p = p_+$ and $p = p_-$. $p = p_+$ (dotted), $p = p_-$ (solid).

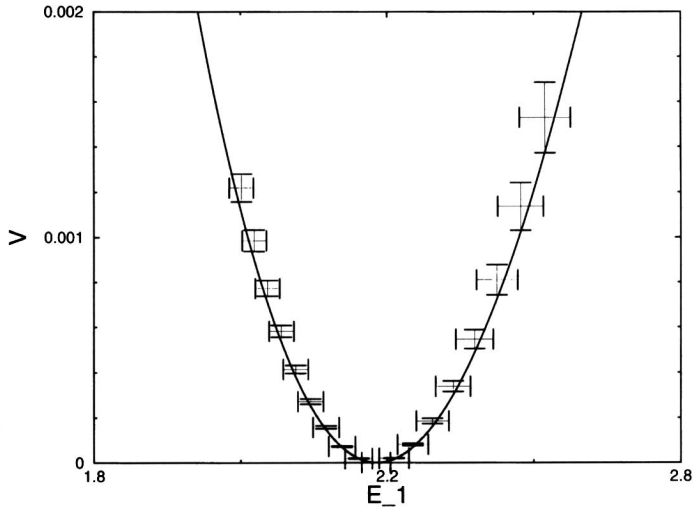

Fig. 30. Effective Potential of E_1 in the nonequilibrium system with the twisted-Gaussian ansatz, $p = p_-$, and with DNS. DNS with error bars.

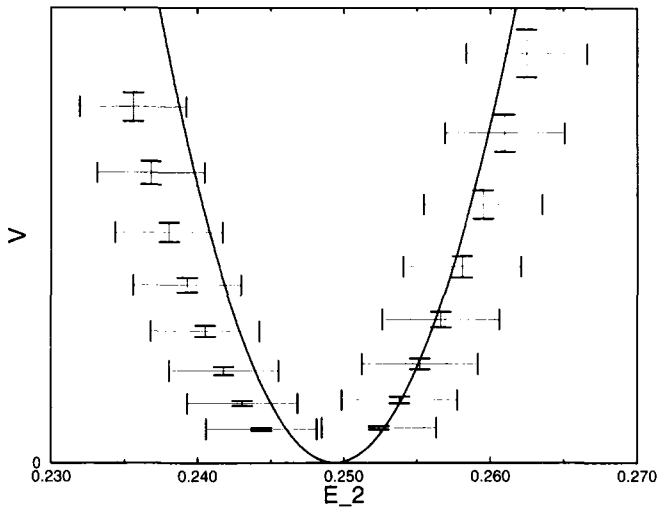

Fig. 31. Effective potential of E_2 in the nonequilibrium system with the twisted-Gaussian ansatz, $p = p_-$, and with DNS. DNS with error bars.

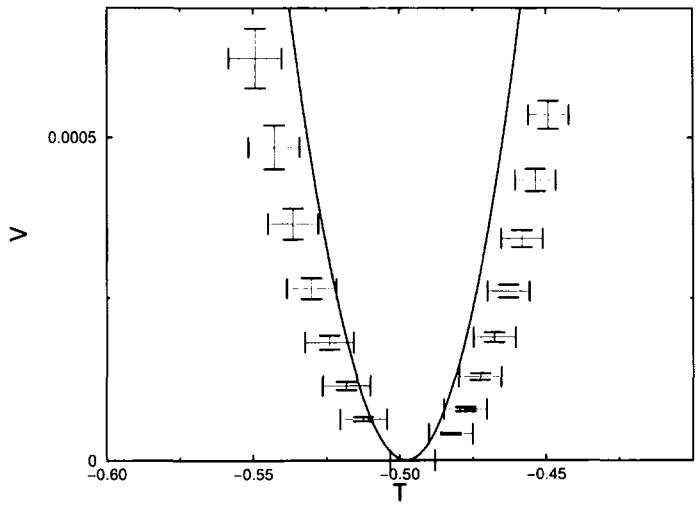

Fig. 32. Effective potential of T in the nonequilibrium system with the twisted-Gaussian ansatz, $p = p_-$, and with DNS. DNS with error bars.

It should be kept in mind that p was the *only* free parameter, adjusted to fit the mean exactly. The agreement away from the mean is thus a success of the TG closure. This is a remarkable success, given that the TG-*Ansatz* succeeds with only 4 parameters whereas the systematic Hermite-expansion *Ansatz* failed to calculate the nonequilibrium potentials even with over 200 parameters! The important general lesson of this example is that a quite accurate calculation of effective potentials is possible by the Rayleigh–Ritz method, even with a few parameter *Ansatz* rather than with a systematic approximation procedure (such as Hermite expansions). This makes it meaningful to compare Rayleigh–Ritz approximate potentials in PDF closures with those obtained from experiment or DNS.

6. CONCLUSIONS

(1) We have proposed in this paper a *refined ergodic hypothesis* for Navier–Stokes turbulence, which can be proved as a theorem in other simpler systems, such as the 3-mode dynamics of Eq. (1). The effective potentials which appear in that hypothesis are subject to realizability conditions: (i) positivity, (ii) unicity of the minimum, and (iii) convexity. These realizability conditions apply to general turbulence statistics, e.g. 1st-order statistics such as mean velocity profiles, and not just to variables like energy whose means must be positive. In the 3-mode system the 1st-order statistics are rather trivial[5] and have not been studied in this work. However, we have considered the effective potentials of a 3rd-order statistic, $T(\mathbf{x}) = x_1 x_2 x_3$, which lacks also a classical realizability constraint. We have further explained how to economically calculate approximations to the effective potentials within PDF-based moment closures. It should be emphasized that the computational work required to calculate a single point on the approximate potential curve in the neighborhood of the minimum is of the same order as the work required in the given closure to calculate the predicted mean value itself. It involves a numerical fixed point problem, Eqs. (30)–(32), of the same type as that considered in calculating the stationary values of the moments, Eq. (19). Hence, there is little extra expense to calculate a few points of the potential curve in the neighborhood of the predicted mean.

(2) We have proposed a *realizability criterion*: predicted means in PDF-closures must be rejected for statistics whose effective potentials calculated within the same closure violate realizability. We have studied the utility of this criterion in the 3-mode system and compared it there with

[5] With a nonzero-mean force, there are nonzero means of x_i in the 3-mode system but the contribution of fluctuations to them is not very important.

other realizability constraints. It is clear that the classical 2nd-moment realizability conditions are too weak. They simply do not apply generally enough, i.e. to arbitrary statistics. Even where they apply, the effective potential realizability conditions are a useful complementary condition. For example, the χ^2-*Ansatz* in the 3-mode system—equivalent there to the quasinormal approximation—predicts all positive energies, but underpredicts E_1 in the cascade state by a factor of 3. However, the χ^2 effective potential of E_1 violates realizability and indicates failure of convergence for that statistic. On the opposite side, the PDF-realizability condition—i.e. the positivity requirement of the whole distribution—is too strong. In the case both of the Hermite-expansion PDF's and the χ^2-*Ansatz*, realizability of the PDF was violated, yet the closures made very accurate predictions nonetheless for certain statistics. Some predictions were indeed badly in error, but the failure of PDF-realizability gave no indication which predictions might be spurious. By contrast, the effective potential realizability conditions have been able in the 3-mode system to discriminate between the good predictions and the bad in several cases. It should be emphasized again that satisfaction of realizability *cannot* imply that the prediction is good, but that failure of realizability should imply that the prediction is poor.

This expectation has been well borne out in the 3-mode system. We regard our work here as a simple case study in the use of the variational principle for modeling purposes. By a combination of physical insight, information from DNS, and exact constraints from the dynamics, PDF closures were formulated to predict the quantities of interest. The realizability conditions on the effective potentials of those statistics were then used as a "screen" or "filter" to eliminate *a priori* the poor predictions. In the present case, predictions which failed to pass the realizability check were generally at least 3–4% from the correct answer and, in most cases, much worse than that. On the other hand, the predictions which passed the realizability check were sometimes very close and sometimes far off. However, even when far off—as the predicted E_1 in the TG *Ansatz* for p near 0 or 1—the closures which satisfied the realizability conditions could here, by adjustment of free parameters, correctly postdict the given statistic. It cannot be concluded from this study that the same will hold in Navier–Stokes turbulence, but we reasonably expect it to be so.

(3) We have also considered an *optimization principle*: the "optimum value" of any free parameter in a PDF closure to "best" predict a given mean statistic ought to be one for which the corresponding effective potential is stationary under variation of the parameter. Although there is a certain theoretical basis, the utility of the optimization principle as a practical

tool is not so clear. In fact, in the 3-mode system its success has been mixed. It worked exceedingly well to select σ for the Hermite-expansion *Ansatz* in the equilibrium case, and it also accelerated convergence for increasing N in the near-equilibrium cascade state. However, it performed rather poorly to select p for the twisted-Gaussian closure in the non-equilibrium cascade state, at large Reynolds number. A basic difficulty is that the stationarity condition is only guaranteed to give the correct potential if one varies over the full, infinite-dimensional set of trial states. Unlike the analogous Rayleigh–Ritz method in quantum mechanics, there is no monotonicity in the approximation. Adding a few parameters to an *Ansatz* may even *worsen* the agreement with the true answer, for any finite number of parameters. For this reason, one cannot be confident that the principle will truly choose the "best" value of the parameters in any finitely-parameterized *Ansatz*. The main virtue of the "minimal sensitivity principle" as an *a priori* selection device is that it can protect one from making far worse choices than the optimal one. Lacking other relevant information, it is therefore a sensible *a priori* selection principle. The greatest benefit appears to occur within convergent approximation schemes, for which the rate of convergence can be substantially accelerated. Further study of this point is required.

(4) In future work we shall make a similar investigation for time-dependent turbulence, where the *effective action* plays an analogous role to the effective potential in the statistical steady-state. We have shown elsewhere[11] that there is a Rayleigh–Ritz algorithm available also to approximate the full effective action functional within PDF closures. The validity of the realizability criterion and optimization principle in that context is an important question in assessing their practical potential. Indeed, many of the flows of greatest engineering interest are statistically time-dependent, e.g. high-Reynolds number flow past an accelerating object. The effective action is also a tool that can be brought to bear in statistical steady states without assuming the refined ergodic hypothesis, which could be false in certain applications. Work in these directions is already in progress.

It is clearly crucial to examine the utility of the novel realizability conditions within PDF closures for realistic systems, such as Navier–Stokes turbulence. Some initial exercises have been carried out, with gratifying results. These include free decay of homogeneous, isotropic turbulence governed by Navier–Stokes dynamics[44] and turbulent advection of a passive scalar.[45] For the method to be practically useful the realizability conditions on the approximate potentials must fall into a certain middle ground. On the one hand, the conditions must be sensitive enough that they detect a significant fraction of poor predictions in advance, but, on the

other hand, they should not be so over-sensitive that they disqualify all but a small number of predictions, many of those rejected being adequate for practical engineering purposes. It remains to be seen whether the proposed new conditions will meet this objective. To establish their utility will ultimately require more than anecdotal studies of particular systems, as here. What is really required is a careful study of a large number of representative flows to establish that the method leads in fact to a statistically-improved predictive ability. However, the present work already gives tantalizing evidence for the method, which offers a real prospect for some *a priori* information in turbulence modeling. We expect that the variational approach will enable turbulence modellers to exploit in a practical way the many advances in theoretical understanding of small-scale turbulence which have been made in recent years. Novel PDF closures can be readily developed within our scheme. In fact, any good guess of the turbulence statistics may be input as a trial *Ansatz* in our variational method.

APPENDIX 1. BACKGROUND ON THE 3-MODE MODEL

The 3-mode stochastic dynamical system is specified by the Eqs. (1)

$$\dot{x}_i = A_i x_j x_k - \nu_i x_i + f_i \tag{102}$$

$i = 1, 2, 3$ which are equivalent for $\nu_i = 0$, $i = 1, 2, 3$ to the Euler equations of solid-body rotation. The variables x_i then represent the components of angular momenta M_i associated with the principal axes, and the A_i are given as

$$A_i = \frac{(I_j - I_k)}{I_j I_k} \tag{103}$$

in terms of the corresponding moments of inertia I_i. f_i has the interpretation of an ith component of imposed torque in the body-frame. Correspondingly, for $\nu_i = f_i = 0$ there are two independent quadratic integrals of motion:

$$E = \tfrac{1}{2}(x_1^2 + x_2^2 + x_3^2) \tag{104}$$

and

$$H = \tfrac{1}{2} A_2 x_1^2 - \tfrac{1}{2} A_1 x_2^2 \tag{105}$$

In the solid-body analogy the first integral E corresponds to one-half the total square angular momentum $M_1^2 + M_2^2 + M_3^3$ and $H + E/I_3$ corresponds

to the rotational kinetic energy $M_1^2/2I_1 + M_2^2/2I_2 + M_3^2/2I_3$. However, in the fluid mechanical interpretation it is instead E that corresponds to *energy*, and we thus use that terminology here. Because there are two integrals of motion and only 3 degrees-of-freedom, the system is exactly integrable and may be solved by quadratures in terms of Jacobi elliptic functions (see refs. 19 and 21, or 46, Section 37). Thus it is necessary in this instance to use random forcing to obtain a well-defined statistics.

When the forces f_i are chosen to be Gaussian and white-noise in time; i.e.

$$\langle f_i(t)\, f_j(t')\rangle = 2\kappa_i\, \delta_{ij}\, \delta(t-t'), \tag{106}$$

then the dynamics is still Markovian and the Liouville (Fokker–Planck) equation is

$$\begin{aligned}\partial_t P(\mathbf{x}, t) &= \sum_{i=1}^{3} \left[-\frac{\partial}{\partial x_i}(A_i X_j x_k - \nu_i x_i) + \kappa_i \frac{\partial^2}{\partial x_i^2} \right] P(\mathbf{x}, t) \\ &\equiv \hat{L} P(\mathbf{x}, t)\end{aligned} \tag{107}$$

It is easily checked that when the *fluctuation-dissipation relation* (FDR),

$$\frac{\kappa_i}{\nu_i} = \Theta \tag{108}$$

for $i = 1, 2, 3$, is imposed, then the equation has as its stationary solution the *absolute equilibrium* distribution

$$P_{eq}(\mathbf{x}) = \frac{1}{(2\pi\Theta)^{3/2}} \exp\left[-\frac{(x_1^2 + x_2^2 + x_3^2)}{2\Theta} \right] \tag{109}$$

The dynamics for this solution is statistically time-reversal invariant, i.e. detailed balance is satisfied, since the equivalent "potential conditions" of ref. 47 are satisfied. Hence, there are no nonvanishing fluxes or irreversible cascades when the FDR is imposed.

However, the stationary states will generically be nonequilibrium flux states when the FDR is not satisfied. To keep the analogy with fluid turbulence, we generally strongly force the mode i with the coefficient A_i of opposite sign as the coefficients A_j, A_k for the other two modes j and k, which are instead strongly damped. In fact, it is well-known that, of the three steady-state solutions of the Euler solid-body equations corresponding to rotations about each of the three principal axes, the rotations around the axes of lowest and highest moments of inertia are stable while

rotation around the axis of middle inertia is unstable (see ref. 48, p. 203). In our work we have always taken $A_1 = 2$, $A_2 = A_3 = -1$. Observe that the 1-mode then corresponds to an unstable, large-scale mode, while 2 and 3-modes correspond to stable small-scale modes. There is an irreversible energy cascade set up from the forced mode-1 into the damped modes-2 and 3. This is reflected in the development of a negative steady-state triple moment, $\langle x_1 x_2 x_3 \rangle < 0$, which is associated with energy transfer out of the 1-mode and into the 2 and 3-modes. Because these steady-states are irreversible statistical equilibria, there are no *a priori* expressions that can be written for them, as for the absolute equilibrium in Eq. (109). We note only that, as a consequence of the statistical invariance of the forces to reflection of sign, $f_i \to -f_i$, independently for each $i = 1, 2, 3$, these steady-state distributions possess a group of symmetries, isomorphic to the Klein *Viergruppe*, generated by the reflections:

$$(x_1, x_2, x_3) \to (-x_1, -x_2, x_3) \tag{110}$$

$$(x_1, x_2, x_3) \to (x_1, -x_2, -x_3) \tag{111}$$

$$(x_1, x_2, x_3) \to (-x_1, x_2, -x_3) \tag{112}$$

Furthermore, when one chooses $\kappa_2 = \kappa_3$, $\nu_2 = \nu_3$, then the steady-state distribution is also invariant under the permutation of 2 and 3-modes:

$$(x_1, x_2, x_3) \to (x_1, x_3, x_2) \tag{113}$$

These statistical symmetries are very helpful in modeling, both to guess suitable PDF *Ansätze* and to reduce the required number of parameters in them.

APPENDIX II. THE OPTIMIZATION IN A PARAMETER

Let $V_*(\mathbf{w}; c)$ be the Rayleigh–Ritz potential in a closure, depending on a free parameter c. Then there is always a trivial stationary value at each $\mathbf{w}$ given as $\langle \mathbf{W} \rangle_{\mu_*(c)}$ for *some* choice of c; i.e. at any mean value of $\mathbf{W}$ attainable within the closure. In fact, c is a stationary value itself at the corresponding $\mathbf{w}$. Let $\bar{\mathbf{w}}_*(c) = \langle \mathbf{W} \rangle_{\mu_*(c)}$ be the closure mean, as a function of the free parameter c. Since $V_*(\bar{\mathbf{w}}_*(c); c) = 0$ it follows by differentiation in c that

$$\left(\frac{\partial V_*}{\partial \mathbf{w}}\right)_c (\bar{\mathbf{w}}_*(c); c) \cdot \frac{d\bar{\mathbf{w}}_*}{dc}(c) + \left(\frac{\partial V_*}{\partial c}\right)_{\mathbf{w}} (\bar{\mathbf{w}}_*(c); c) = 0 \tag{114}$$

for all c. However,

$$\left(\frac{\partial V_*}{\partial \mathbf{w}}\right)_c (\bar{\mathbf{w}}_*(c); c) = \mathbf{h}_*(\bar{\mathbf{w}}_*(c); c) = \mathbf{0} \tag{115}$$

Thus, it follows from Eqs. (114)–(115) that

$$\left(\frac{\partial V_*}{\partial c}\right)_{\mathbf{w}} (\mathbf{w}; c) = 0 \tag{116}$$

if $\mathbf{w} = \bar{\mathbf{w}}_*(c)$, as claimed. However, it is also then true that $V_*(\mathbf{w}; c) = 0$, so that if that value of c were substituted as the "optimum value" at each $\mathbf{w}$, then the resulting potential would be $= 0$ whenever $\mathbf{w} = \bar{\mathbf{w}}_*(c)$ for some choice of c!

The difficulty with this, obviously, is that c is a *constant* parameter in the PDF, and the stationary point, if it exists, must be the same value c_* for all values of $\mathbf{w}$, i.e. Eq. (116) must hold simultaneously for *all* $\mathbf{w}$ with a single c_*. It can be easily seen that Eq. (116) holds for *all* $\mathbf{w}$ with $c = c_*$ only if

$$\left(\frac{\partial \mathbf{w}_*}{\partial c}\right)_{\mathbf{h}} (\mathbf{h}; c_*) = 0 \tag{117}$$

for all $\mathbf{h}$. Indeed, differentiating Eq. (116) with respect to $\mathbf{w}$ at $c = c_*$, it follows that

$$\left(\frac{\partial \mathbf{h}_*}{\partial c}\right)_{\mathbf{w}} (\mathbf{w}; c_*) = 0 \tag{118}$$

Furthermore, differentiating $\mathbf{w}_*(\mathbf{h}_*(\mathbf{w}; c); c) = \mathbf{w}$ with respect to c gives

$$\left(\frac{\partial \mathbf{w}_*}{\partial \mathbf{h}}\right)_c (\mathbf{h}_*(\mathbf{w}; c); c) \cdot \left(\frac{\partial \mathbf{h}_*}{\partial c}\right)_{\mathbf{w}} (\mathbf{w}; c) + \left(\frac{\partial \mathbf{w}_*}{\partial c}\right)_{\mathbf{h}} (\mathbf{h}_*(\mathbf{w}; c); c) = \mathbf{0} \tag{119}$$

for all $\mathbf{w}$ and c. Putting $c = c_*$ and using Eq. (118) for that value, one obtains Eq. (117). In particular, this equation must be true for $\mathbf{h} = \mathbf{0}$. This means that

$$\frac{d\bar{\mathbf{w}}_*}{dc} (c_*) = 0 \tag{120}$$

is a *necessary condition* that c_* be a stationary point for the entire function $V_*(\mathbf{w}; c)$. It is therefore interesting to consider such special parameter

values c_* of the closure where the means obey Eq. (120), since these are the candidates to be *optimum values* for the variation of $V_*(\mathbf{w}; c)$. Observe that these have an interesting interpretation as the points of *minimal sensitivity*[32] of the means $\bar{\mathbf{w}}_*(c)$ to variation of c. If such a value of c_* were to exist and, further, give a stationary point of $V_*(\mathbf{w}; c)$, then that value would be the optimal value of the parameter c according to the variational principle. Notice that, while c_* must be a constant for each variable $\mathbf{W}$ of the system, the constant *may* be distinct for different choices of $\mathbf{W}$.

APPENDIX III. PERTURBED DYNAMICAL VECTORS IN THE CLOSURES

We list here the perturbed vectors fields $\bar{\mathbf{V}}(\bar{\boldsymbol{\mu}}, \mathbf{h})$ used in the closures to calculate the approximate effective potentials V_{E_1}, V_{E_2} and V_T. We have denoted as $\mathbf{h} = (h_{E_1}, h_{E_2}, h_T)$ the perturbation field parameters for each of the three random variables considered. From the $\bar{\mathbf{V}}$-vector the $\mathbf{A}$-matrix is easily calculated as in Eq. (29) by differentiation with respect to $\bar{\boldsymbol{\mu}}$.

III.1. Hermite-Expansion Ansatz

The perturbed vector field corresponding to moment index $\mathbf{n}$ is given here by

$$V_{\mathbf{n}}(\boldsymbol{\mu}, \mathbf{h}) = \sum_{\mathbf{m}} L_{\mathbf{h}}(\mathbf{n}; \mathbf{m})\, \boldsymbol{\mu}_{\mathbf{m}} \tag{121}$$

where

$$L_{\mathbf{m}}(\mathbf{n}; \mathbf{m}) = L(\mathbf{n}; \mathbf{m}) + h_{E_1} E_1(\mathbf{n}; \mathbf{m}) + h_{E_2} E_1(\mathbf{n}; \mathbf{m}) + h_T T(\mathbf{n}; \mathbf{m}) \tag{122}$$

with $L(\mathbf{n}; \mathbf{m})$ already given by Eq. (46), and with

$$\begin{aligned} E_i(\mathbf{n}; \mathbf{m}) = \tfrac{1}{2}\sigma_i^2 [& \sqrt{(n_i+2)(n_i+1)}\, \delta_{n_i+2,\, m_i} + (2n_i+1)\, \delta_{n_i,\, m_i} \\ & + \sqrt{n_i(n_i-1)}\, \delta_{n_i-2,\, m_i}] \times \delta_{n_j,\, m_j}\, \delta_{n_k,\, m_k} \end{aligned} \tag{123}$$

for i, j, k a cyclic permutation of 1, 2, 3 and

$$T(\mathbf{n}; \mathbf{m}) = \prod_{i=1}^{3} \sigma_i [\sqrt{n_i+1}\, \delta_{n_i+1,\, m_i} + \sqrt{n_i}\, \delta_{n_i-1,\, m_i}] \tag{124}$$

III.2. Chi-Square Ansatz

To simplify notation we introduce another field h_{E_3} corresponding to $E_3(\mathbf{x}) = \frac{1}{2}x_3^2$. We then have for $i = 0$:

$$V_0(\boldsymbol{\mu}, \mathbf{h}) = \frac{1}{2}\sum_{i=1}^{3} h_{E_i}\mu_i + h_T\mu_4 \tag{125}$$

for $i = 1, 2, 3$:

$$\begin{aligned} V_i(\boldsymbol{\mu}, \mathbf{h}) = {} & (2A_i\mu_4 - 2\nu_i\mu_i + 2\kappa_i) + \tfrac{3}{2}h_{E_i}(\mu_i^2 + 2\mu_4^{4/3}) \\ & + \tfrac{1}{2}\sum_{j\neq i} h_{E_j}(\mu_i\mu_j + 2\mu_4^{4/3}) + h_T(3\mu_i\mu_4 + 6\mu_4^{5/3}) \end{aligned} \tag{126}$$

and, for $i = 4$,

$$\begin{aligned} V_4(\boldsymbol{\mu}, \mathbf{h}) = {} & (A_1\mu_2\mu_3 + A_2\mu_1\mu_3 + A_3\mu_1\mu_2 - (\nu_1 + \nu_2 + \nu_3)\mu_4) \\ & + \frac{3}{2}\sum_i h_{E_i}(\mu_i\mu_4 + 2\mu_4^{5/3}) + h_T(\mu_1\mu_2\mu_3 + 2(\mu_1 + \mu_2\mu_3)\mu_4^{4/3} + 20\mu_4^2) \end{aligned} \tag{127}$$

III.3. Twisted-Gaussian Ansatz

For $i = 0$;

$$V_0(\boldsymbol{\mu}, \mathbf{h}) = \tfrac{1}{2}h_{E_1}\mu_1 + \tfrac{1}{2}h_{E_2}\mu_2 + h_T\mu_3 \tag{128}$$

for $i = 1$:

$$V_1(\boldsymbol{\mu}, \mathbf{h}) = (2A_1\mu_3 - 2\nu_1\mu_1 + 2\kappa_1) + \tfrac{3}{2}h_{E_1}\mu_1^2 + \tfrac{1}{2}h_{E_2}\mu_1\mu_2 + 2h_T\mu_1\mu_3 \tag{129}$$

for $i = 2$:

$$\begin{aligned} V_2(\boldsymbol{\mu}, \mathbf{h}) = {} & (2A_2\mu_3 - 2\nu_2\mu_2 + 2\kappa_2) + \tfrac{1}{2}h_{E_1}\mu_1\mu_2 \\ & + \frac{3h_{E_2}}{8pq}\left(\mu_2^2 + \frac{\pi\mu_3^2}{2|\mu_1|} + (p-q)\sqrt{2\pi}\,|\mu_1|^{-1/2}\mu_2\mu_3\right) \\ & + \frac{3h_T}{2p}\left(\mu_2\mu_3 + \frac{1}{\sqrt{2\pi}}|\mu_1|^{1/2}\mu_2^2 + \sqrt{\frac{\pi}{8}}\,|\mu_1|^{-1/2}\mu_3^2\right) \end{aligned} \tag{130}$$

and, for $i=3$,

$$V_3(\boldsymbol{\mu}, \mathbf{h}) = \frac{3A_1}{4pq}\left(\mu_2^2 + \frac{\pi\mu_3^2}{2\,|\mu_1|} + (p-q)\sqrt{2\pi}\,|\mu_1|^{-1/2}\mu_2\mu_3\right)$$
$$+ (A_2 + A_3)\,\mu_1\mu_2 - (\nu_1 + \nu_2 + \nu_3)\,\mu_3$$
$$+ h_{E_1}\mu_1\mu_3 + \frac{3h_{E_2}}{2p}\left(\mu_2\mu_3 + \frac{1}{\sqrt{2\pi}}\,|\mu_1|^{1/2}\mu_2^2 + \sqrt{\frac{\pi}{8}}\,|\mu_1|^{-1/2}\mu_3^2\right)$$
$$+ \frac{3h_T}{4pq}\left(\mu_1\mu_2^2 + \operatorname{sign}(\mu_1)\frac{\pi}{2}\mu_3^2 + (p-q)\sqrt{2\pi}\operatorname{sign}(\mu_1)\,|\mu_1|^{1/2}\mu_2\mu_3\right) \tag{131}$$

ACKNOWLEDGMENTS

The authors wish to thank B. Bayly, S. Girimaji, R. H. Kraichnan, C. D. Levermore, and Y. Oono for helpful conversations on the subject of this paper. FJA thanks W. Klein for his encouragement and financial support. FJA was funded in part by NSF Grant DMR 9633385. All numerical computations were performed at the Center for Computational Science of Boston University and at the University of Arizona, Department of Mathematics.

REFERENCES

1. J. Boussinesq, "Essai sur la théorie des eaux courantes," *Mém. prés. par div. savantes à l'Acad. Sci.* (Paris) **23**:1 (1877).
2. O. Reynolds, "On the dynamical theory of incompressible viscous fluids and the determination of the criterion," *Phil. Trans. Roy. Soc. Lond.* **186**:123 (1894).
3. C. G. Speziale, "Analytical methods for the development of Reynolds-stress closures in turbulence," *Ann. Rev. Fluid Mech.* **23**:107 (1991).
4. R. H. Kraichnan, "A theory of turbulence dynamics," in: *Second Symposium on Naval Hydrodynamics, 29–44* (Office of Naval Research, Washington, D.C., 1958), Ref. ACR-38.
5. R. H. Kraichnan, "Dynamics of nonlinear stochastic systems," *J. Math. Phys.* **2**:124 (1961).
6. R. H. Kraichnan, "Realizability inequalities and closed moment equations," *Ann. N. Y. Acad. Sci.* **357**:37 (1980).
7. U. Schumann, "Realizability of Reynolds-stress turbulence models," *Phys. Fluids* **20**:721 (1977).
8. J. L. Lumley, "Computational modeling of turbulent flows," *Adv. Appl. Mech.* **18**:123 (1978).
9. L. Onsager, "Reciprocal relations in irreversible processes," (I) *Phys. Rev.* **37**:405 (1931); (II) **38**:2265 (1931).
10. G. L. Eyink, "Turbulence noise," *J. Stat. Phys.* **83**:955 (1996).

11. G. L. Eyink, "Action principle in nonequilibrium statistical dynamics," *Phys. Rev. E* **54**:3419 (1996).
12. H. Chen, S. Chen, and R. H. Kraichnan, "Probability distribution of a stochastically advected scalar field," *Phys. Rev. Lett.* **65**:575 (1990).
13. T. Gotoh and R. H. Kraichnan, "Statistics of decaying Burgers turbulence," *Phys. Fluids A* **5**:445 (1992).
14. D. C. Haworth and S. B. Pope, "A generalized Langevin model for turbulent flows," *Phys. Fluids* **29**:387 (1986).
15. S. B. Pope, "Lagrangian PDF methods for turbulent flows," *Ann. Rev. Fluid Mech.* **26**:23 (1994).
16. R. O. Fox, "The Fokker–Planck closure for turbulent molecular mixing: passive scalars," *Phys. Fluids A* **4**:1230 (1992).
17. F. J. Alexander and G. L. Eyink, "Rayleigh–Ritz calculation of effective potential far from equilibrium," *Phys. Rev. Lett.* **78**:1 (1997).
18. F. J. Alexander and G. L. Eyink, "Turbulence fluctuations and new universal realizability conditions in modeling," *Phys. Rev. Lett.* **78**:2563 (1997).
19. E. Lorenz, "Maximum simplification of the dynamic equations," *Tellus* **12**:243 (1960).
20. R. H. Kraichnan, "Direct-interaction approximation for a system of several interacting simple shear waves," *Phys. Fluids* **6**:1603 (1963).
21. R. H. Kraichnan, "Invariance principles and approximations in turbulence dynamics," in *Dynamics of Fluids and Plasmas*, S. I. Pai, ed. (Academic Press, New York, 1966), pp. 239–255.
22. S. A. Orszag and L. R. Bissonnette, "Dynamical properties of truncated Wiener–Hermite expansions," *Phys. Fluids* **10**:2603 (1967).
23. A. Juneja, D. P. Lathrop, K. R. Sreenivasan, and G. Stolovitsky, "Synthetic turbulence," *Phys. Rev. E* **49**:5179 (1994).
24. A. S. Monin and A. M. Yaglom, *Statistical Fluid Mechanics*, Vol. I (The MIT Press, Cambridge, MA, 1971).
25. U. Frisch, *Turbulence* (Cambridge U. Pr., Cambridge, 1995).
26. S. R. S. Varadhan, *Large Deviations and Applications* (SIAM, Philadelphia, 1984).
27. Y. Takahashi, "Entropy functional (free energy) for dynamical systems and their random perturbations," *Proc. Taniguchi Symp. on Stochastic Analysis* (Kinokuniya-North-Holland, Tokyo, 1984).
28. Y. Kifer, "Large deviations in dynamical systems and stochastic processes," *Trans. Am. Math. Soc.* **321**:505 (1990).
29. B. Mandelbrot, "Random multifractals: negative dimensions and the resulting limitations of the thermodynamic formalism," *Proc. Roy. Soc. Lond. A* **434**:79 (1991).
30. B. A. Finlayson, *The Method of Weighted Residuals and Variational Principles* (Academic Press, New York, 1972).
31. F. J. Alexander and G. L. Eyink, "Numerical computation of nonequilibrium effective potential and effective action by constrained Rayleigh–Ritz," unpublished.
32. P. M. Stevenson, "Optimized perturbation theory," *Phys. Rev. D* **23**:2916 (1981).
33. S. F. Edwards, "The statistical dynamics of homogeneous turbulence," *J. Fluid. Mech.* **18**:239 (1964).
34. H. Grad, "On the kinetic theory of rarefied gases," *Comm. Pure and Appl. Math.* **2**:331 (1949).
35. G. L. Eyink, "Hermite-expansion PDF models and second-order closures for homogeneous turbulence," unpublished (1996).
36. M. Abramowitz and L. Stegun, *Handbook of Mathematical Functions* (National Bureau of Standards, Washington, D.C., 1964).

37. Y. Saad, *Numerical Methods for Large Eigenvalue Problems* (Halsted Press, New York, 1992).
38. R. B. Lehoucq, D. C. Sorenson, and C. Yang, *ARPACK USERS GUIDE: Solution of Large Scale Eigenvalue Problems by Implicitly Restarted Arnoldi Methods.* Available at the web-address *ftp://ftp.caam.rice.edu/pub/people/sorenson/ARPACK/*
39. B. Bayly, "Parametric probability distribution function closures," preprint (1992).
40. I. Proudman and W. H. Reid, "On the decay of a normally distributed and homogeneous turbulent velocity field," *Phil. Trans. Roy. Soc. A* **247**:163 (1954).
41. Y. Ogura, "Energy transfer in an isotropic turbulent flow," *J. Geophy. Res.* **67**:3143 (1962).
42. Y. Ogura, "A consequence of the zero-fourth-order-cumulant approximation in the decay of isotropic turbulence," *J. Fluid Mech.* **16**:38 (1963).
43. G. Sochos, "Theoretical and numerical studies of some problems in reaction-diffusion equations, electromagnetic and statistical modeling of turbulent flows," Ph.D. Thesis (Program in Applied Mathematics, University of Arizona, 1994).
44. G. L. Eyink, "Fluctuations in the irreversible decay of turbulent energy." *Phys. Rev. E* **56**:5413 (1997).
45. G. L. Eyink, "A statistical Rayleigh–Ritz study of passive scalar decay: analytical results," unpublished.
46. L. D. Landau and E. M. Lifshitz, *Mechanics* (Pergamon Press, Oxford, 1960).
47. R. Graham and H. Haken, "Generalized thermodynamic potential for markoff systems in detailed balance and far from thermal equilibrium," *Z. Phys.* **243**:289 (1971).
48. C. M. Bender and S. A. Orszag, *Advanced Mathematical Methods for Scientists and Engineers* (Academic, New York, 1978).